Visible Derivative Spectroscopy of Multispectral and Hyperspectral Images: A New Approach to Algal and Cyanobacterial Differentiation

Dr. Joseph Ortiz

(jortiz@kent.edu),

Kent State University

Department of Geology

Collaborators: D. Avouris (KSU), Stephen Schiller (SDSU), Jeff Luvall (NASA-Marshall), John Lekki, RogerTokars, Robert Anderson, Robert Shuchman, Michael Sayers, and Richard Becker

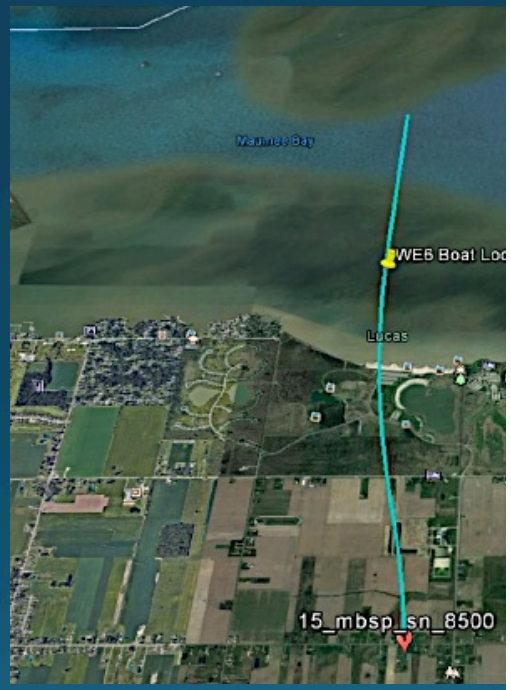

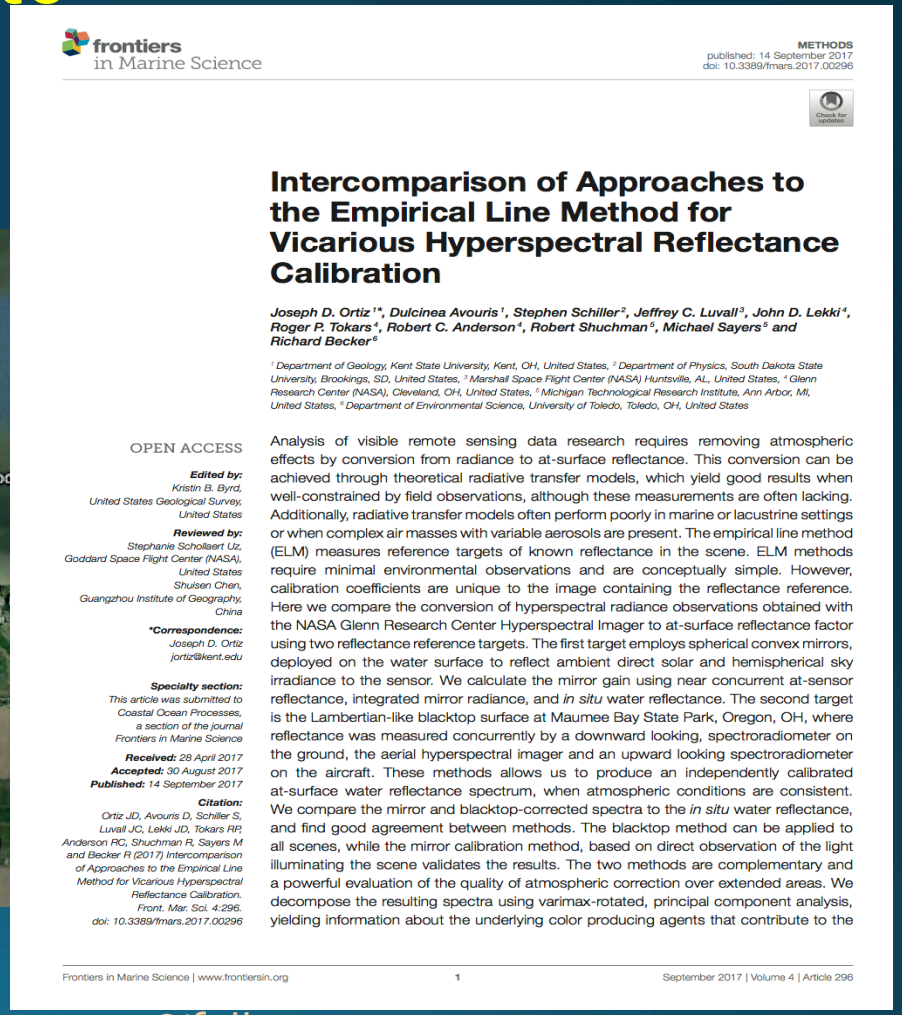

frontiers in Marine Science

METHODS
published: 14 September 2017
doi: 10.3389/fmars.2017.00296

Intercomparison of Approaches to the Empirical Line Method for Vicarious Hyperspectral Reflectance Calibration

Joseph D. Ortiz[1], Dulcinea Avouris[1], Stephen Schiller[2], Jeffrey C. Luvall[3], John D. Lekki[4], Roger P. Tokars[4], Robert C. Anderson[4], Robert Shuchman[5], Michael Sayers[5] and Richard Becker[6]*

[1] Department of Geology, Kent State University, Kent, OH, United States, [2] Department of Physics, South Dakota State University, Brookings, SD, United States, [3] Marshall Space Flight Center (NASA) Huntsville, AL, United States, [4] Glenn Research Center (NASA), Cleveland, OH, United States, [5] Michigan Technological Research Institute, Ann Arbor, MI, United States, [6] Department of Environmental Science, University of Toledo, Toledo, OH, United States

OPEN ACCESS

Edited by:
Kristin B. Byrd,
United States Geological Survey,
United States

Reviewed by:
Stephanie Schollaert Uz,
Goddard Space Flight Center (NASA),
United States
Shulsen Chen,
Guangzhou Institute of Geography,
China

***Correspondence:**
Joseph D. Ortiz
jortiz@kent.edu

Specialty section:
This article was submitted to Coastal Ocean Processes, a section of the journal Frontiers in Marine Science

Received: 28 April 2017
Accepted: 30 August 2017
Published: 14 September 2017

Citation:
Ortiz JD, Avouris D, Schiller S, Luvall JC, Lekki JD, Tokars RP, Anderson RC, Shuchman R, Sayers M and Becker R (2017) Intercomparison of Approaches to the Empirical Line Method for Vicarious Hyperspectral Reflectance Calibration. Front. Mar. Sci. 4:296. doi: 10.3389/fmars.2017.00296

Analysis of visible remote sensing data research requires removing atmospheric effects by conversion from radiance to at-surface reflectance. This conversion can be achieved through theoretical radiative transfer models, which yield good results when well-constrained by field observations, although these measurements are often lacking. Additionally, radiative transfer models often perform poorly in marine or lacustrine settings or when complex air masses with variable aerosols are present. The empirical line method (ELM) measures reference targets of known reflectance in the scene. ELM methods require minimal environmental observations and are conceptually simple. However, calibration coefficients are unique to the image containing the reflectance reference. Here we compare the conversion of hyperspectral radiance observations obtained with the NASA Glenn Research Center Hyperspectral Imager to at-surface reflectance factor using two reflectance reference targets. The first target employs spherical convex mirrors, deployed on the water surface to reflect ambient direct solar and hemispherical sky irradiance to the sensor. We calculate the mirror gain using near concurrent at-sensor reflectance, integrated mirror radiance, and *in situ* water reflectance. The second target is the Lambertian-like blacktop surface at Maumee Bay State Park, Oregon, OH, where reflectance was measured concurrently by a downward looking, spectroradiometer on the ground, the aerial hyperspectral imager and an upward looking spectroradiometer on the aircraft. These methods allows us to produce an independently calibrated at-surface water reflectance spectrum, when atmospheric conditions are consistent. We compare the mirror and blacktop-corrected spectra to the *in situ* water reflectance, and find good agreement between methods. The blacktop method can be applied to all scenes, while the mirror calibration method, based on direct observation of the light illuminating the scene validates the results. The two methods are complementary and a powerful evaluation of the quality of atmospheric correction over extended areas. We decompose the resulting spectra using varimax-rotated, principal component analysis, yielding information about the underlying color producing agents that contribute to the

Peer-Reviewed article: https://www.frontiersin.org/articles/10.3389/fmars.2017.00296/full

Thanks to…

Funding :

✧ Old Woman Creek NERR, Ohio Sea Grant, NASA Glenn, Ohio Board Higher Education

Research Access:

✧ USGS, Ohio EPA, NOAA, ODNR Watercraft Division, Cleveland Water

Collaborators:

✧ NASA Glenn (Lekki, Tokars, Ansari, Liou), OhioView Institutions (Becker, Simic, Wei, Liu)

✧ USGS LEBS (Richard Kraus)

✧ NASA MSFC (Jeff Luvall), SDSU (Stephen Schiller)

✧ NOAA GLERL/MTRI (Leshkevich, Shuchman)

✧ Donna Witter, Sapphire Geoscience Informatics

✧ Khalid Adem Ali, College of Charleston

✧ Sushma Parab, KSU Postdoc

✧ Nick Tufillaro and Curtis Davis, Theo Dreher

  ✧ Hyperspectral Imager for Coastal Oceanography (HICO) Oregon State University

✧ Mandy Razzano, Ohio EPA

✧ Students: N. Bonini, Dulci Avouris, R. Craine, J. Sadallah, N. Wijikoon, D. Fuecht, K. Hollister and others

Ortiz et al., (HyspIRI 2017; jortiz@kent.edu)

Water Quality Monitoring by Remote Sensing? The problem…

- Remote sensing of lake color gives information on plant biomass, but…
- Lake water is a complex "organic soup"
  - Various types of algae and cyanobacteria
  - Colored dissolved organic matter
  - Suspended sediment
- Collect Hyperspectral swaths in Western basin of Lake Erie using NASA Glenn HSI2
- Apply KSU Spectral decomposition method
  - Varimax-rotated, Principal Component Analysis
  - Eigenvector-eigenvalue decomposition
  - Soft unsupervised classification method

Ortiz et al., (HyspIRI 2017; jortiz@kent.edu)

We apply 4 different variations on the Empirical Line Method (ELM) method to reflectance :

ELM0 method uses two instruments (HSI2 and ASD HH2) along with mirrors. Ratio HSI2 water pixels to mirror pixels to remove the atm. Then rescale using ASD HH2 data.

ELM2 method uses two instruments (HSI2 and ASD HH2) surface measurements of reflectance, diffuse to global ratio, and radiative transfer theory to get slope and intercept for water surface and mirror surface pair to go from radiance to reflectance.

The ELM1 method is ELM2 with the intercept term removed to test sensitivity of the VPCA to path radiance impact

The MTRI (Michigan Technological Research Institute) correction method uses three instruments (HSI2, upward looking ASD HH2, and downward looking HH2) The HSI2 and upward looking ASDHH2 provide at-sensor reflectance and then the downward looking HH2 uses a blacktop reference spectra to reshape the at-sensor reflectance to at-surface reflectance

Because the Varimax-rotated, Principal Component Analysis (VPCA) method is based on spectral shapes, it should be relatively insensitive to the quality of the atmospheric correction

ELM method Reflectance and VPCA

- Apply 4 variations of the Empirical Line Method for Atm correction
- How sensitive is the VPCA method to differences in atmospheric correction?

A)

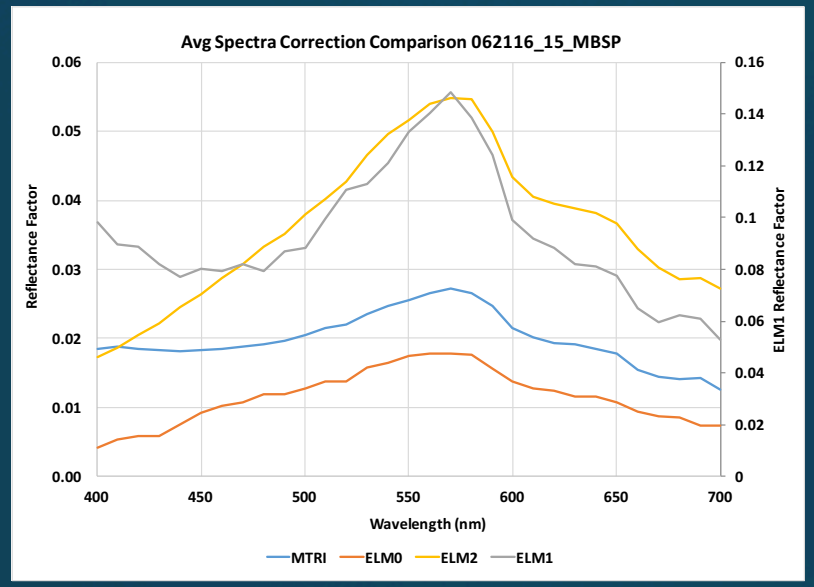

B)

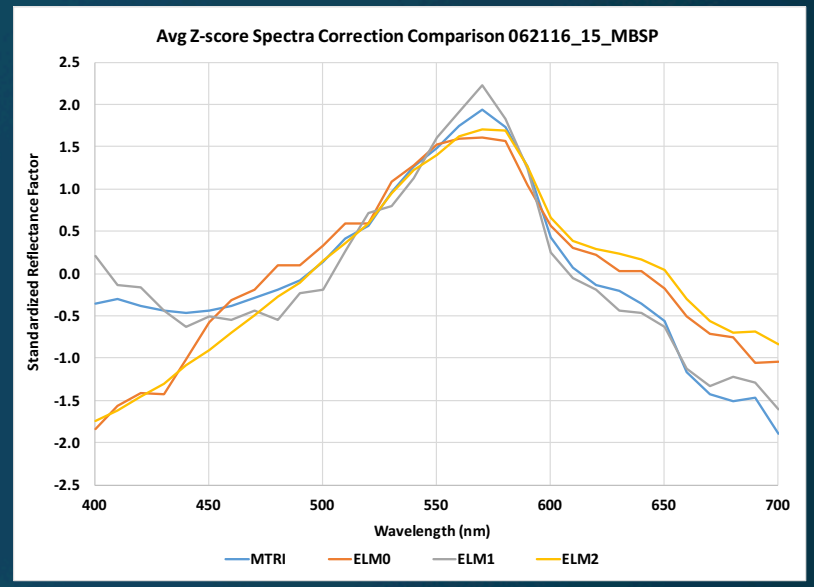

C)

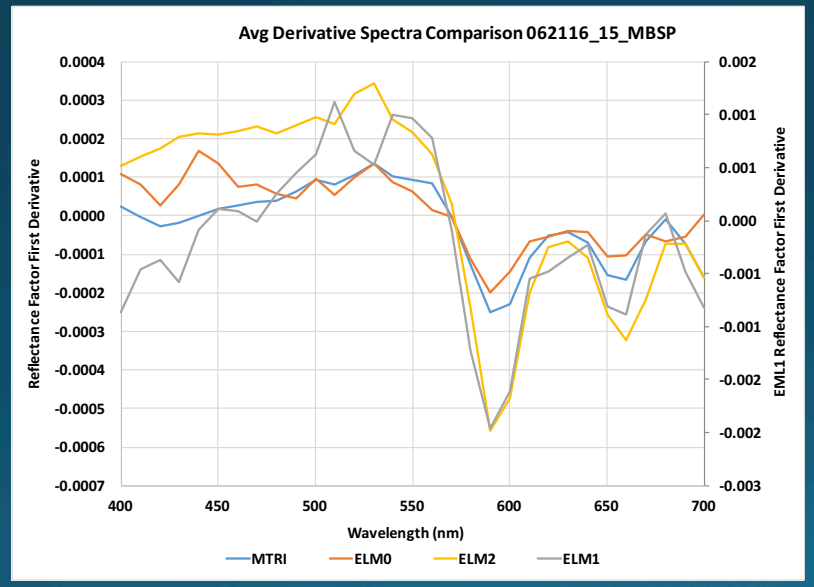

D)

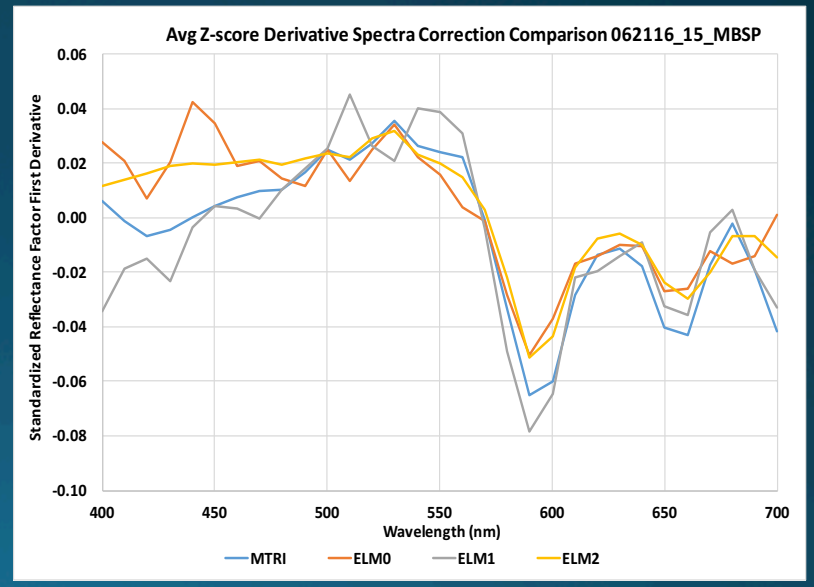

Figure 7

Ortiz et al., (HyspIRI 2017; jortiz@kent.edu)

Figure 8

062116 15_MBSP (10nm, SPEAR0, smooth9, various reflectance transform, georef) VPCA Pattern A

A) Uncorrected RGB (radiance)

B) NOAA CI

C) MTRI 6VPCA 1: 56%

D) ELM0 5VPCA 1: 67.1%

E) ELM1 4VPCA -1: 36.9%

F) ELM2 4VPCA -1: 36.9%

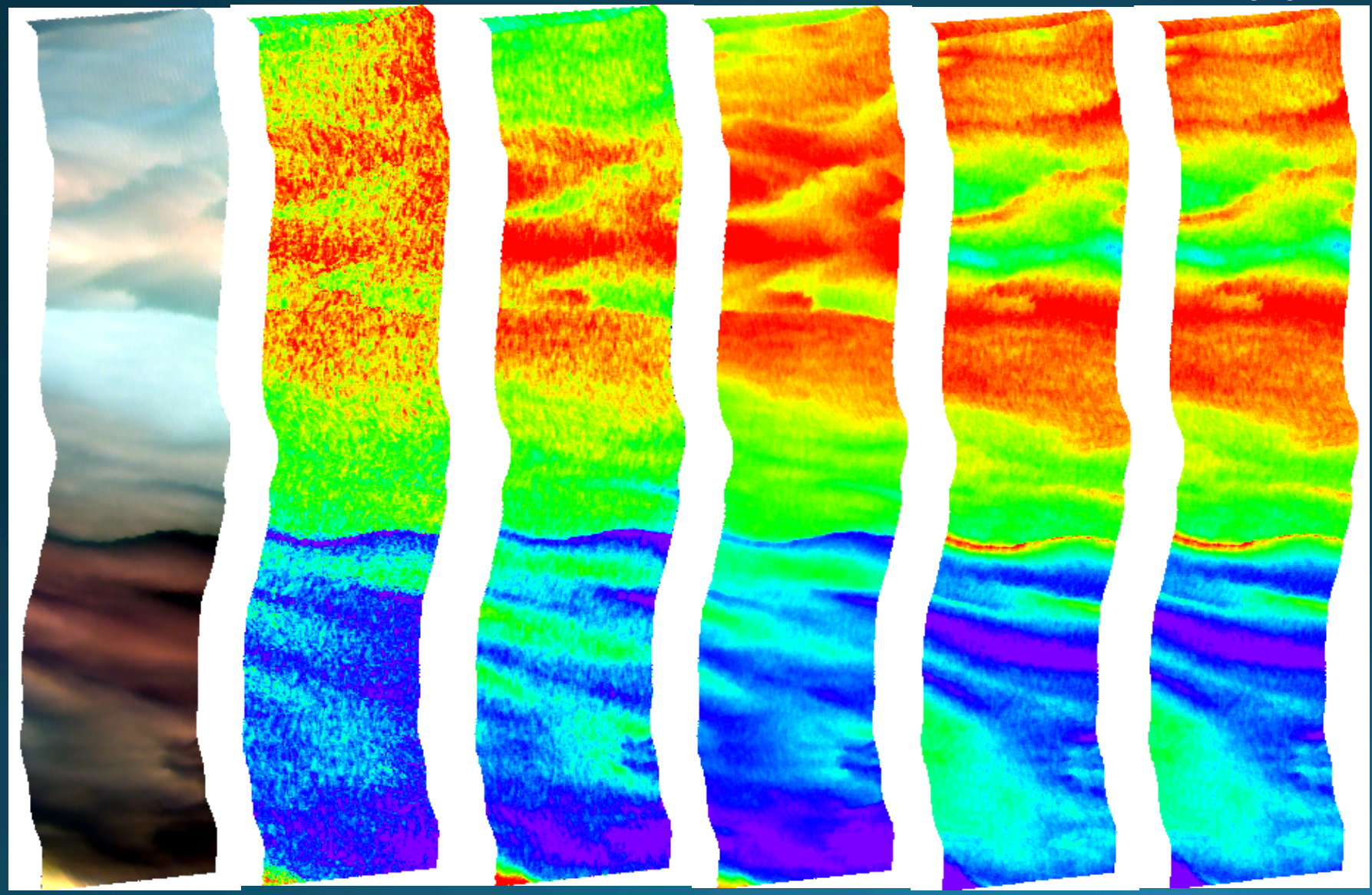

G) Pattern A Loadings

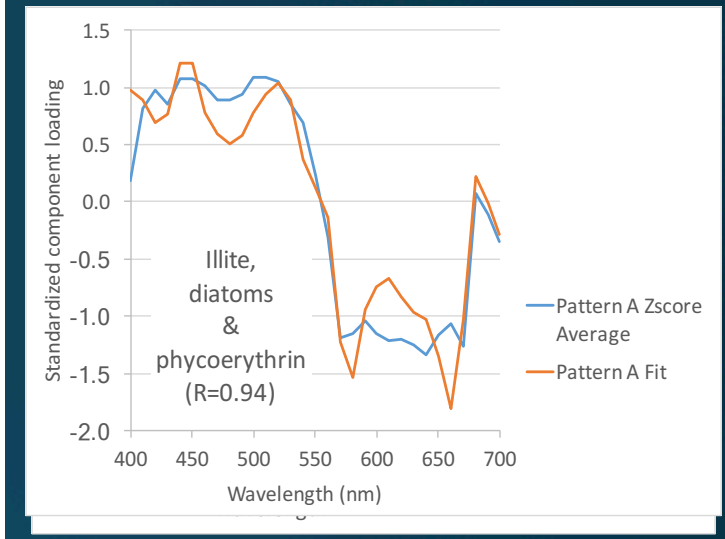

N

Ortiz et al., (HyspIRI 2017; jortiz@kent.edu)

Figure 9

062116 HSI2 Swath 15_MBSP: Pattern B

A) MTRI 6VPCA 2: 16.4%

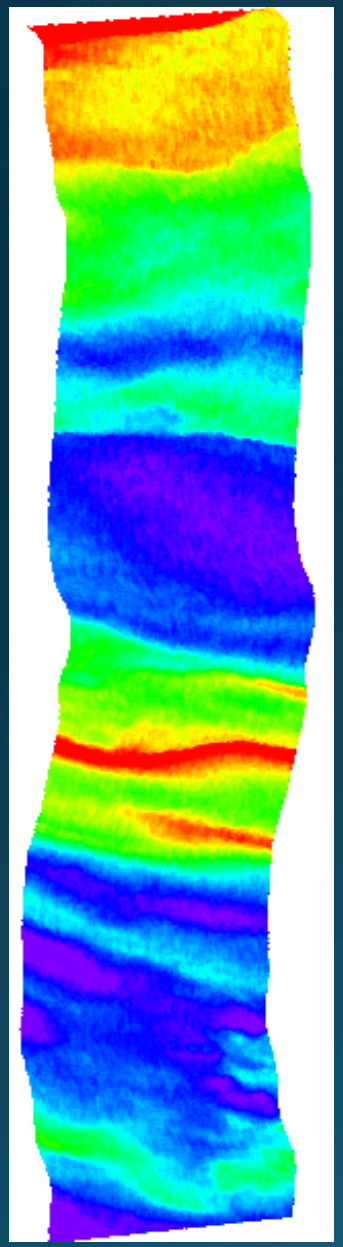

B) ELM0 5VPCA 2: 15.5%

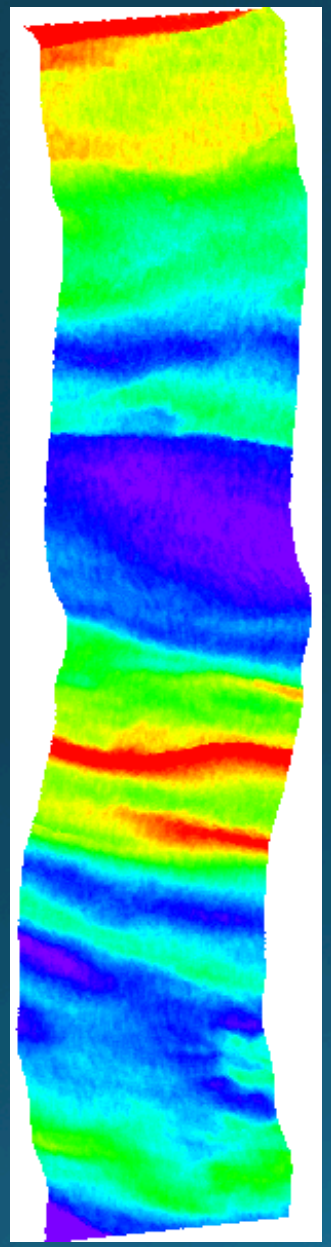

C) ELM1 4VPCA 3: 26.3%

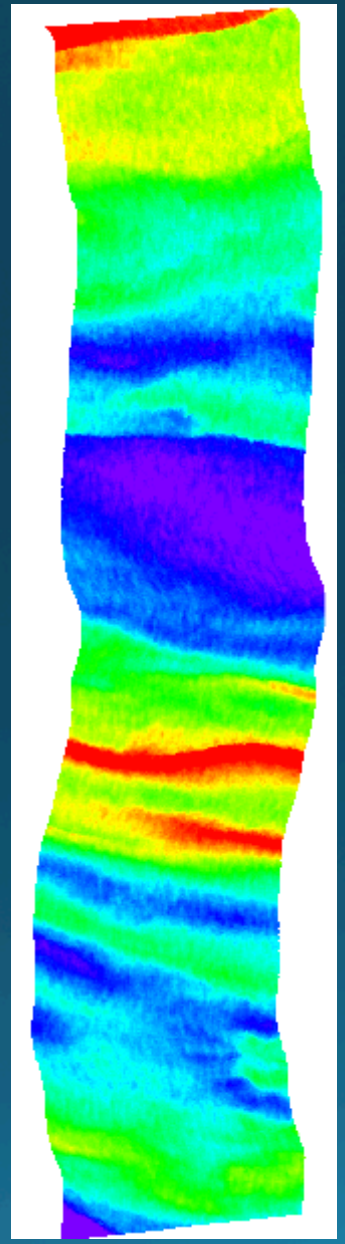

D) ELM2 4VPCA 3: 26.3%

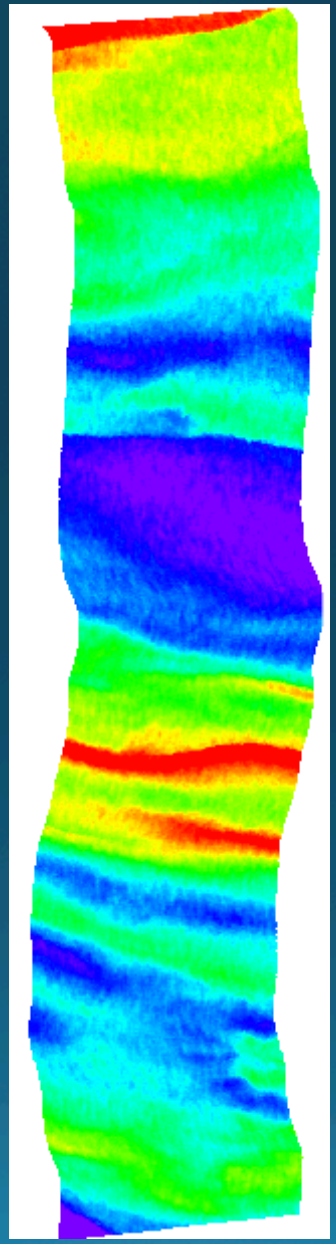

E) Pattern B Loadings

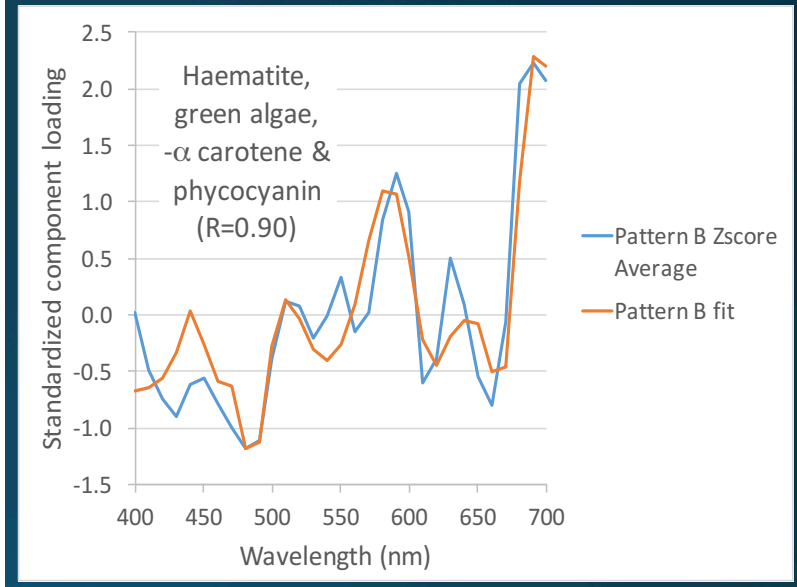

N

Ortiz et al., (HyspIRI 2017; jortiz@kent.edu)

Figure 10

062116 HSI2 Swath 15_MBSP: Pattern C

A) MTRI 6VPCA -3: 10%

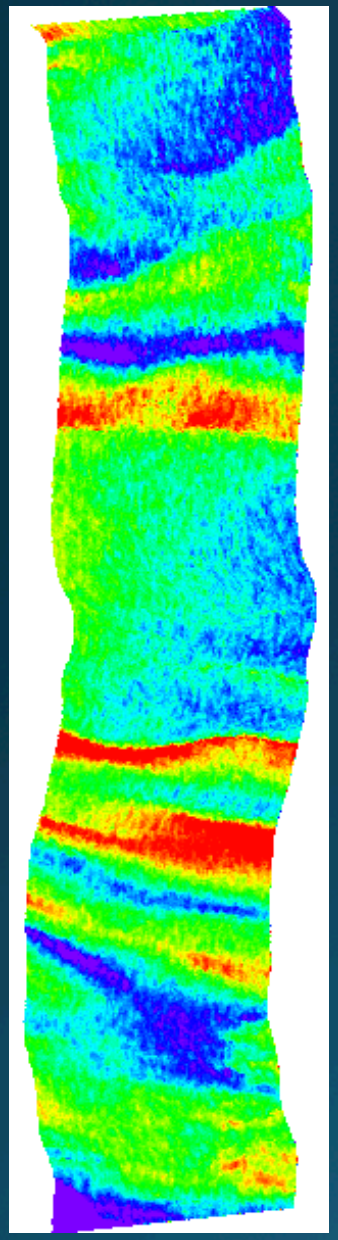

B) ELM0 5VPCA 3: 7.2%

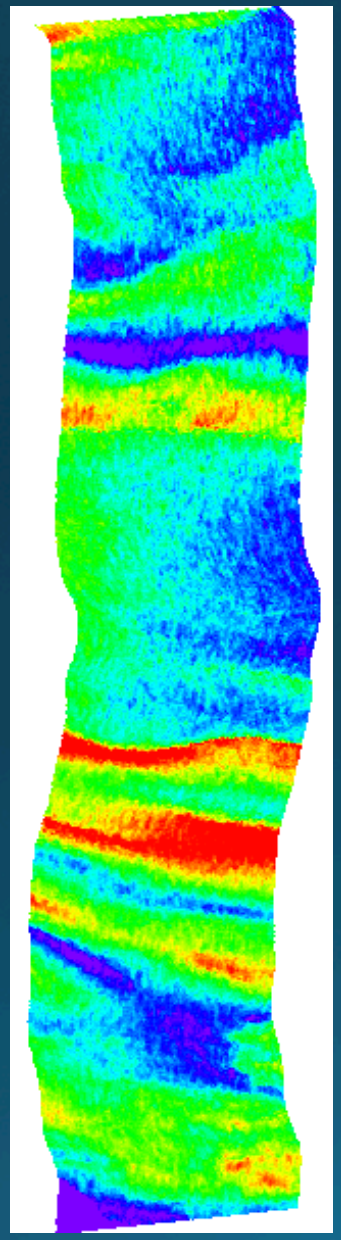

C) ELM1 4VPCA 2: 26.5%

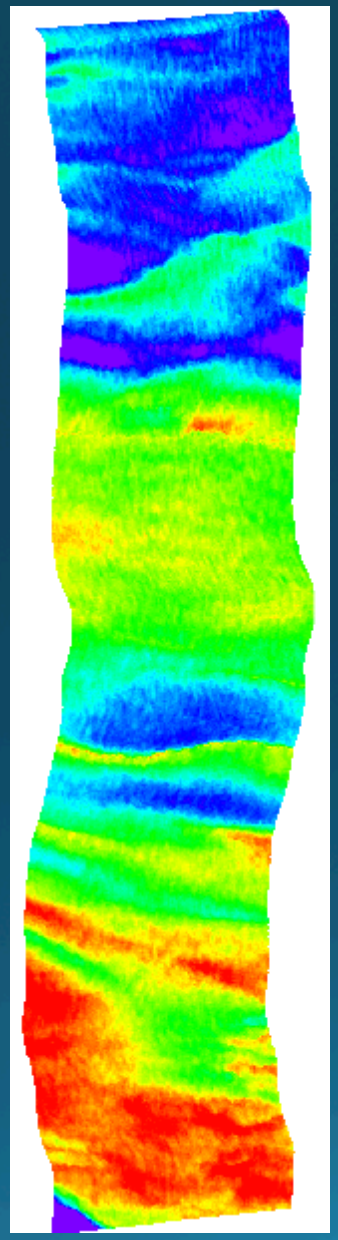

D) ELM2 4VPCA 2: 26.5%

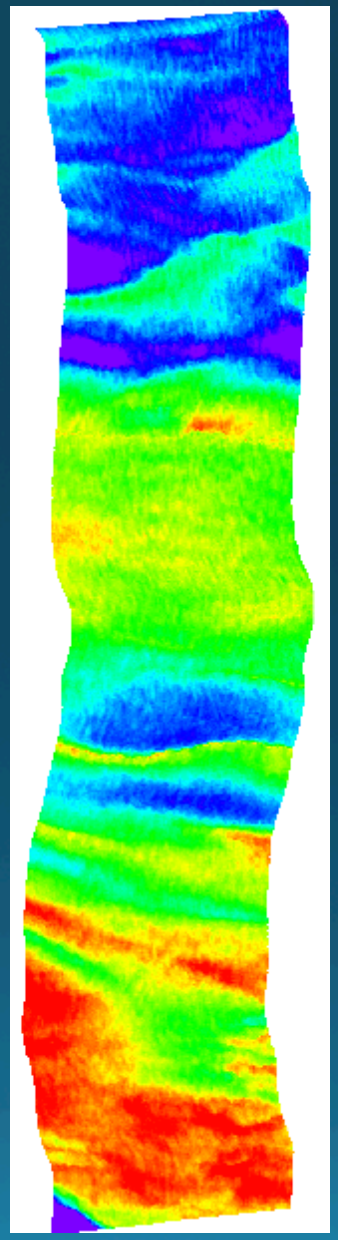

E) Pattern C Loadings

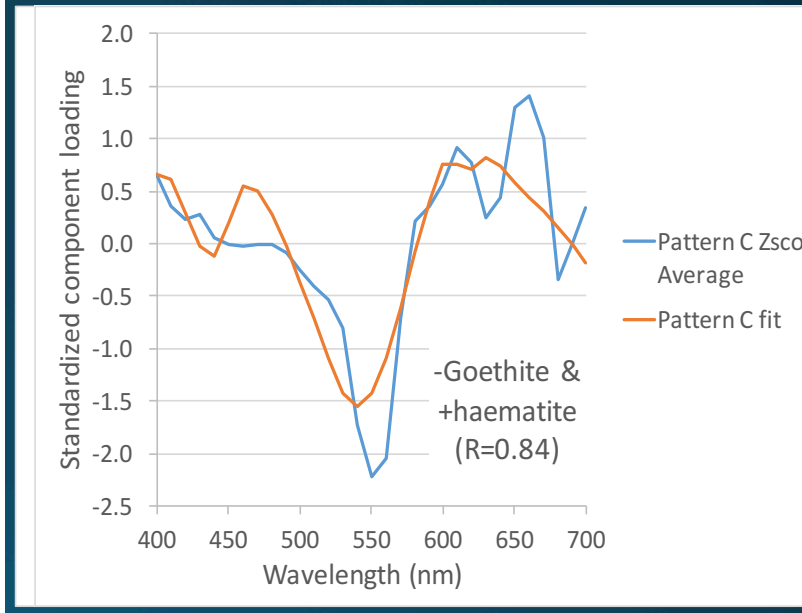

N

Ortiz et al., (HyspIRI 2017; jortiz@kent.edu)

Figure 11

062116 HSI2 Swath 15_MBSP: Pattern D

A) MTRI 6VPCA -4: 7.8%

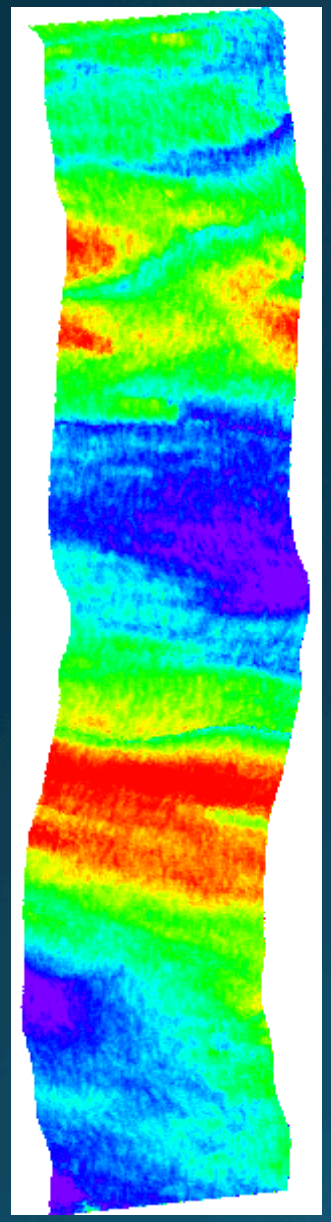

B) ELM0 5VPCA 4: 6.4%

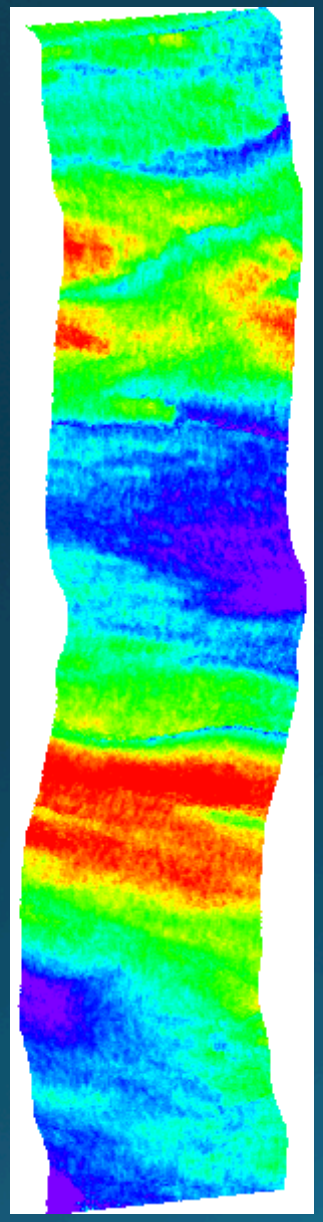

C) ELM1 4VPCA

NO Component with Pattern D

D) ELM2 4VPCA

NO Component with Pattern D

E) Pattern D Loadings

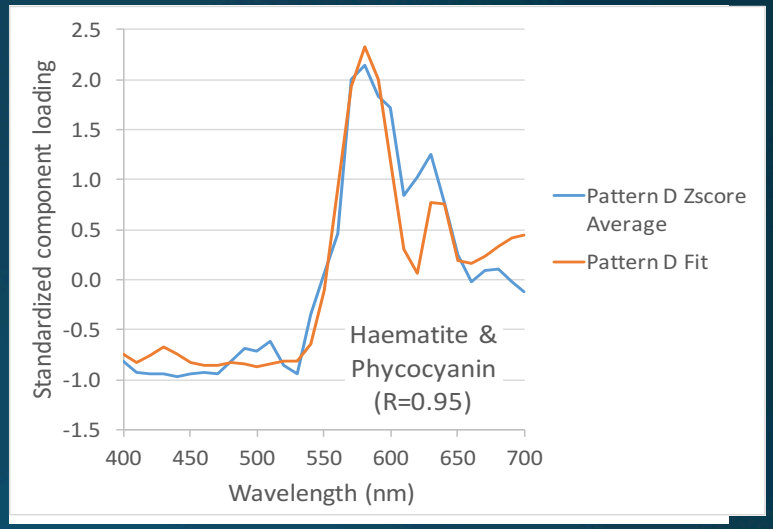

N

Ortiz et al., (HyspIRI 2017; jortiz@kent.edu)

Figure 13

062116 HSI2 Swath 15_MBSP: Pattern F

A) MTRI 6VPCA 6: 1.3%

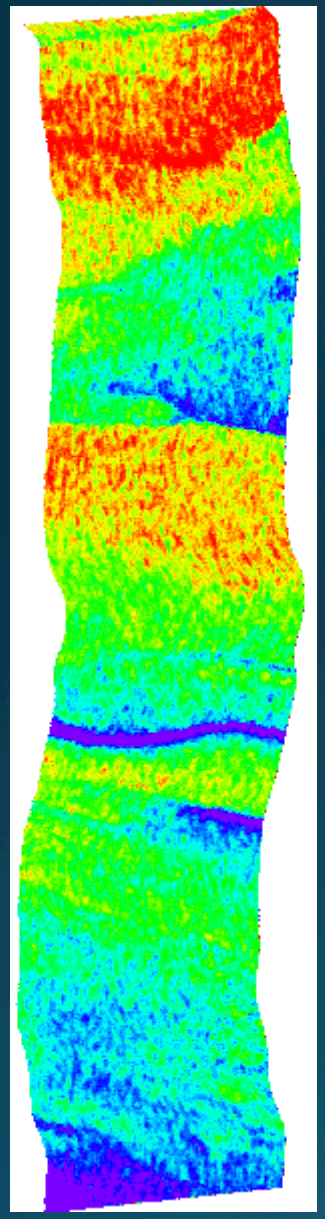

B) ELM0 5VPCA 5: 1%

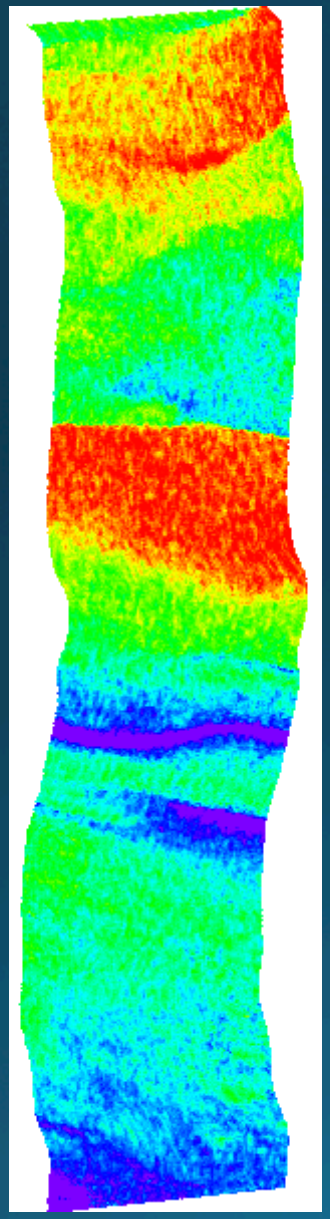

C) ELM1 4VPCA

NO Component with Pattern F

D) ELM2 4VPCA

NO Component with Pattern F

E) Pattern F Loadings

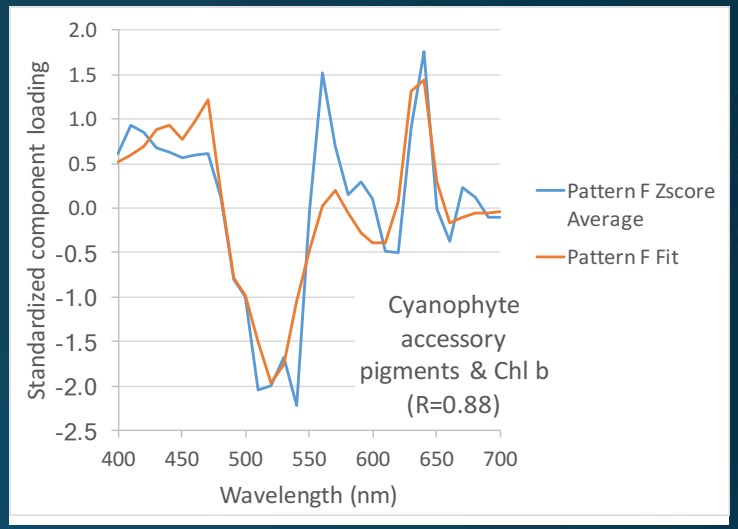

N

Ortiz et al., (HyspIRI 2017; jortiz@kent.edu)

Figure 12

062116 HSI2 Swath 15_MBSP: Pattern E

A) MTRI 6VPCA 5: 4.4%

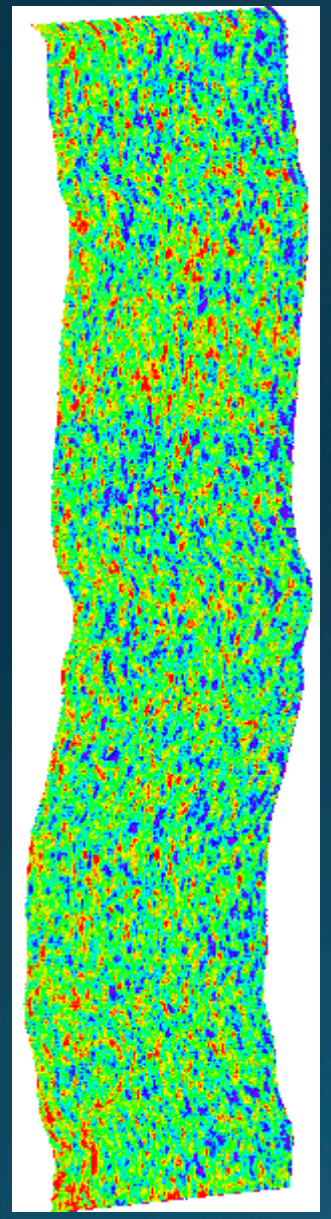

B) ELM0 5VPCA

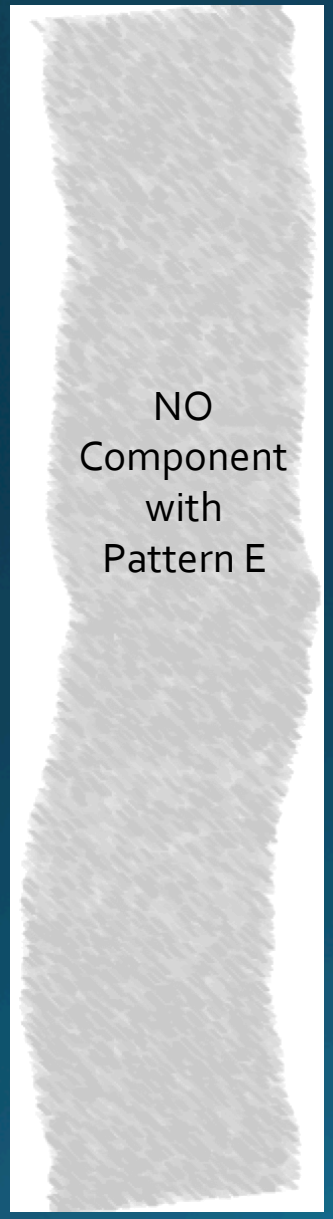

C) ELM1 4VPCA -4: 4.2%

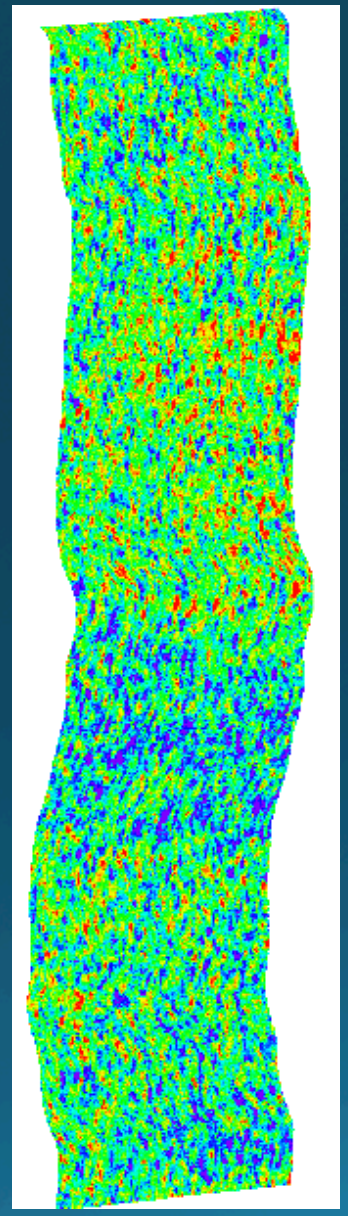

D) ELM2 4VPCA -4: 4.2%

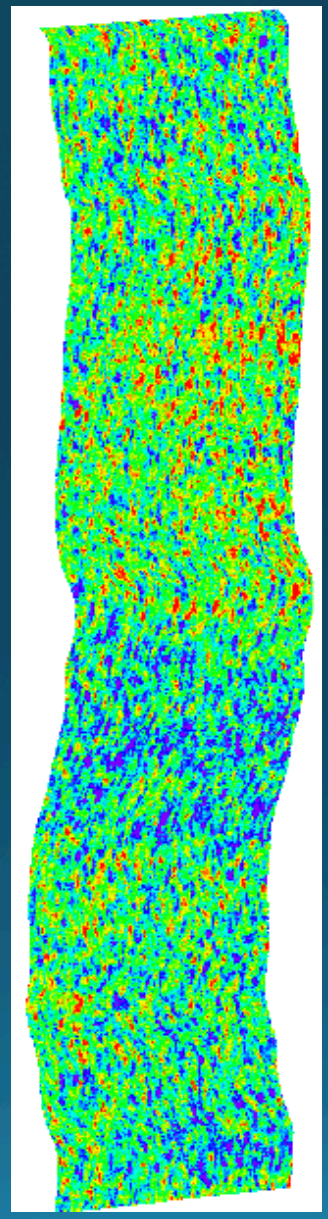

E) Pattern E Loadings

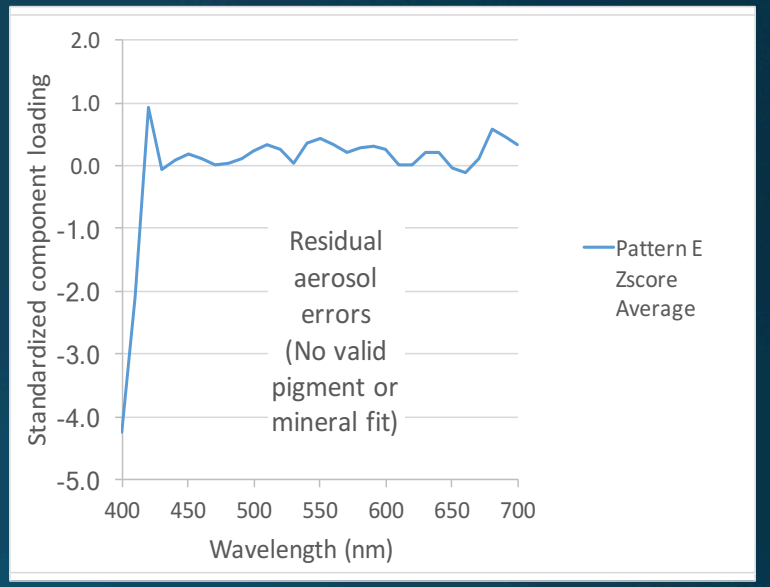

N

Ortiz et al., (HyspIRI 2017; jortiz@kent.edu)

Dealing with Mixed Pixels

Q: How does the amount of information we can extract from Landsat 8 compare with Hyperspectral data sets?

A: Test w/ KSU Spectral decomposition method

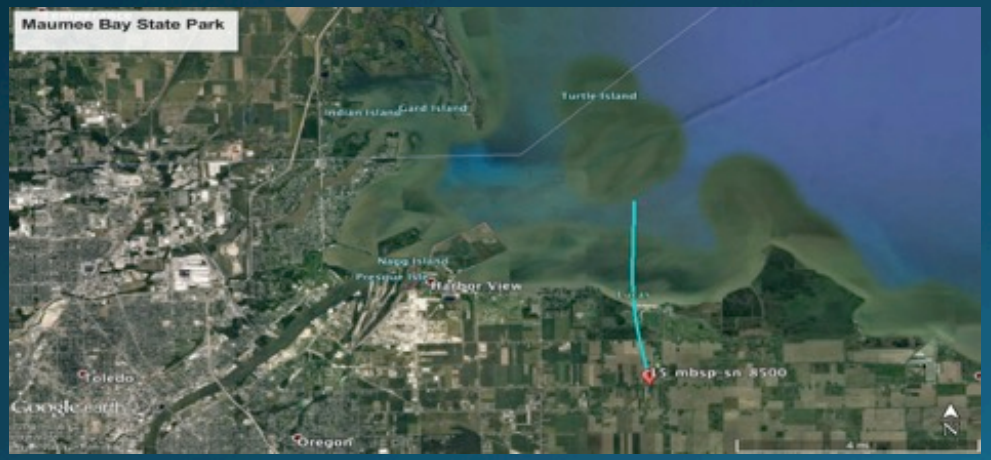

Ortiz et al., (HyspIRI 2017; jortiz@kent.edu)

062116 HSI2 15_MBSP: SPEARo; MTRIcorr; L8 band res; L8 ground res

HSI2 Swath 15_MBSP at Landsat 8 band resolution, HSI2 ground resolution (3m). RGB

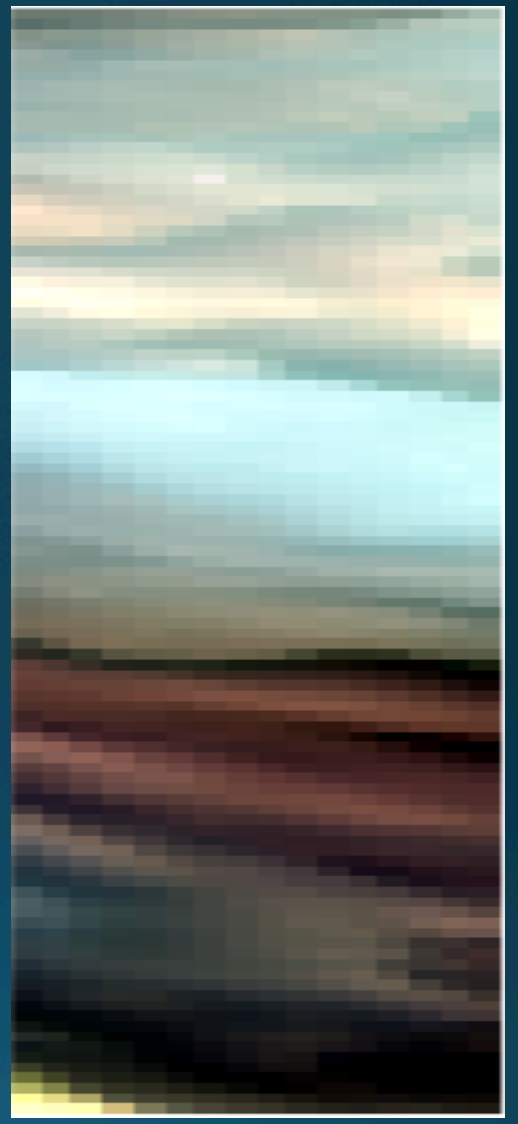

HSI2 Swath 15_MBSP at Landsat 8 band and ground (30m) resolution. RGB of resampled data

A)

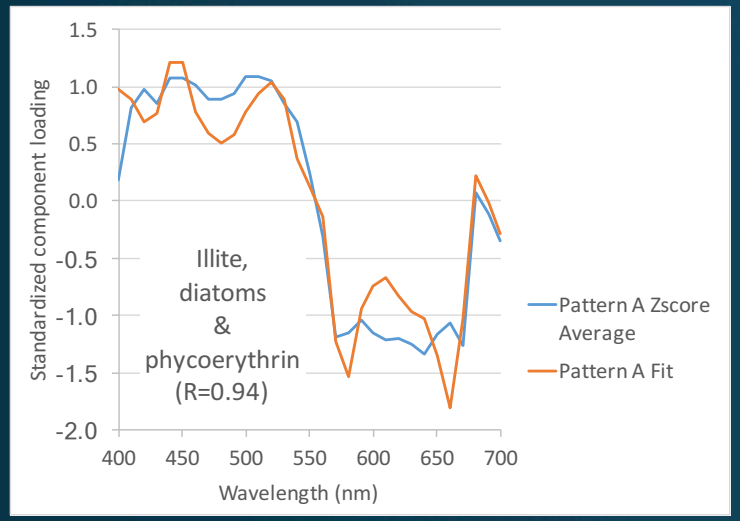

B)

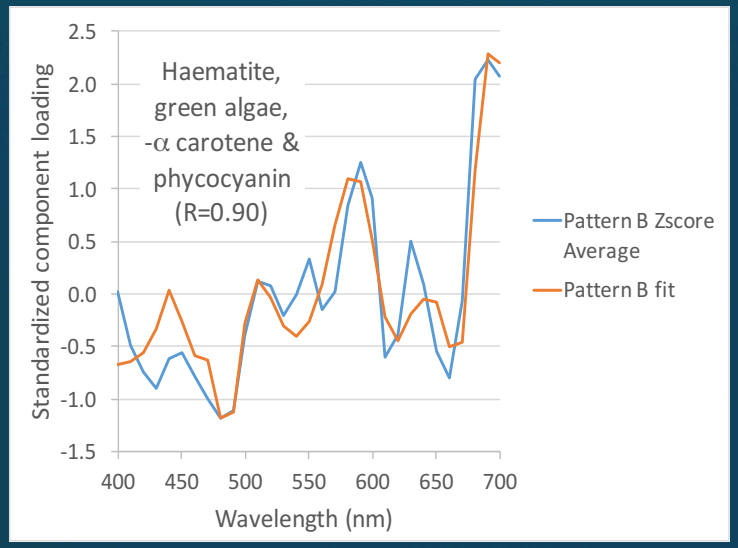

C)

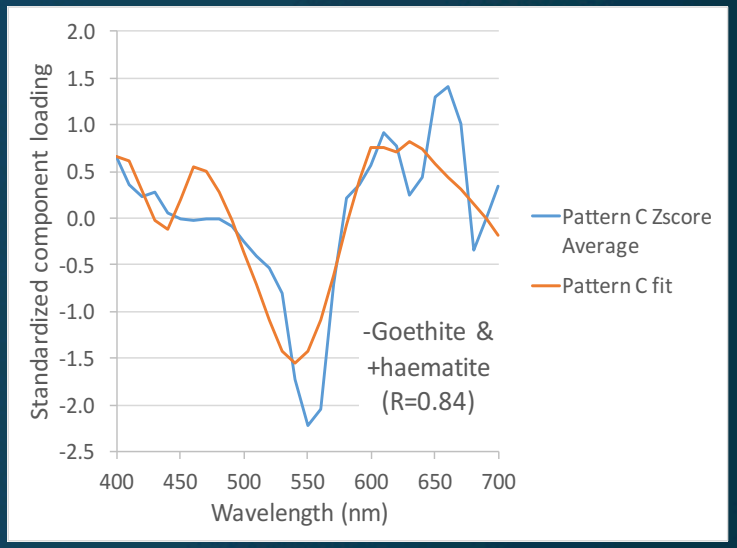

D)

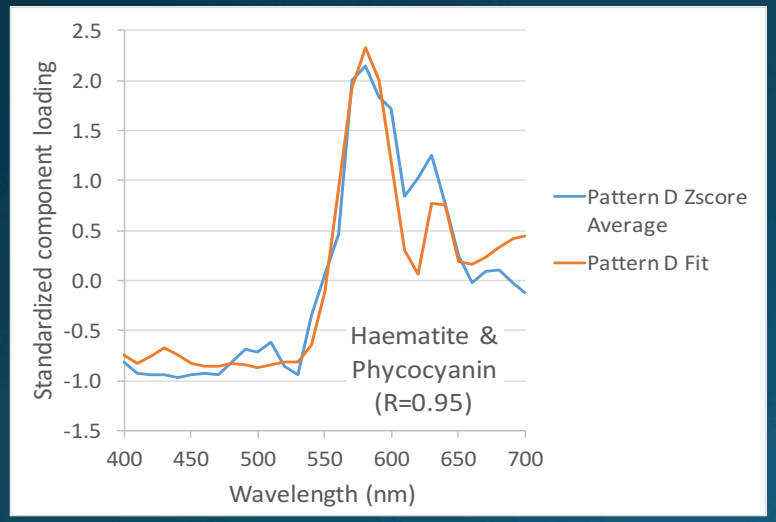

E)

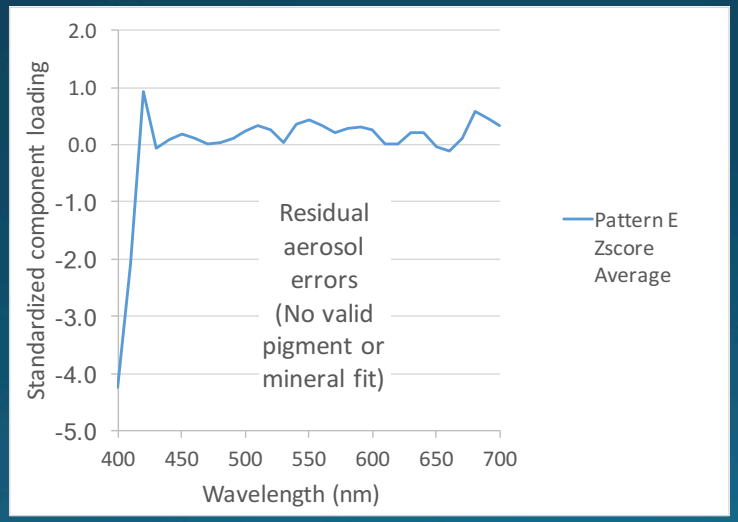

F)

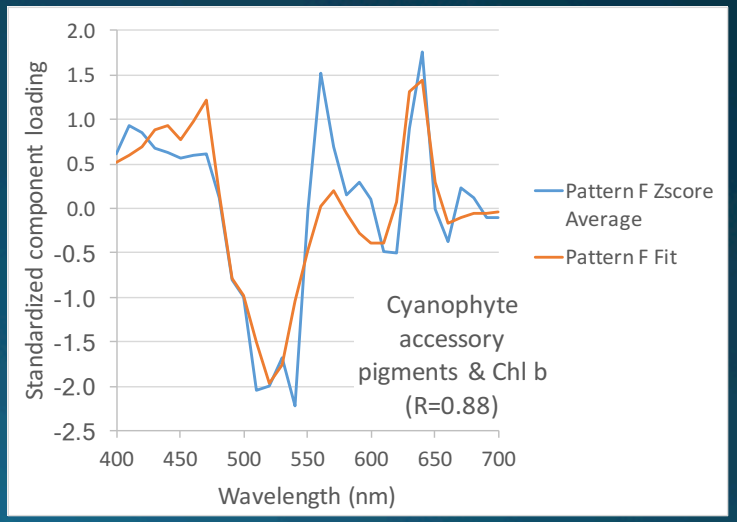

Figure 14 Z-score Loadings

Ortiz et al., (HyspIRI 2017; jortiz@kent.edu)

KSU Spectral Unmixing Experimental Design		
Spectral Placement and Resolution	**Spatial Resolution**	
Landsat 8: Four bands: 440, 480, 560, 655 @ 20, 60, 60 and 30 nm resolution	30 m (simulated)	3 m (simulated)
NASA HSI2: 31 Bands 400-700 nm @10nm resolution	30 m (simulated)	3 m

Ortiz et al., (HyspIRI 2017; jortiz@kent.edu)

062116 HSI2 swath 15: SPEAR0; MTRIcorr; 10nm; 3m – smooth9 pixels: **5VPCA**

A) RGB

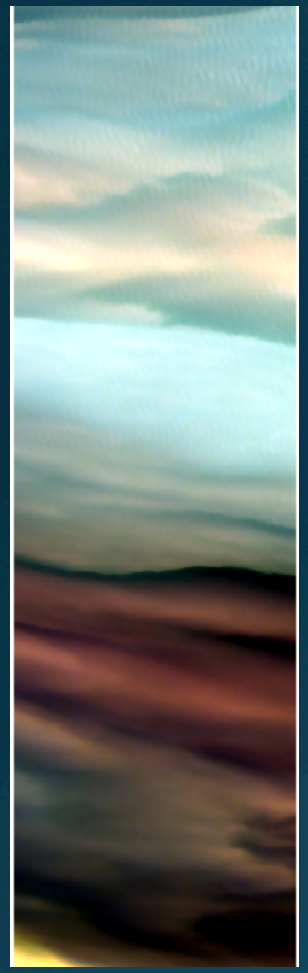

B) MTRI 6VPCA 1: 55.8%

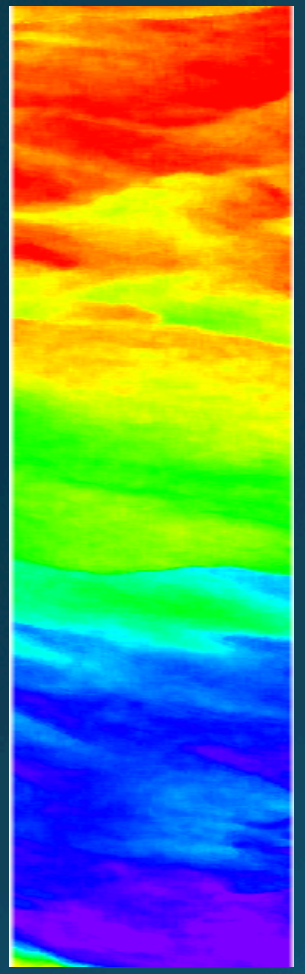

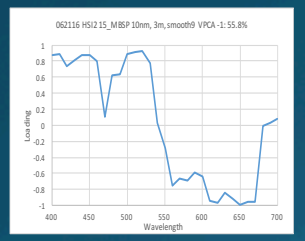

C) MTRI 6VPCA 2: 24.9%

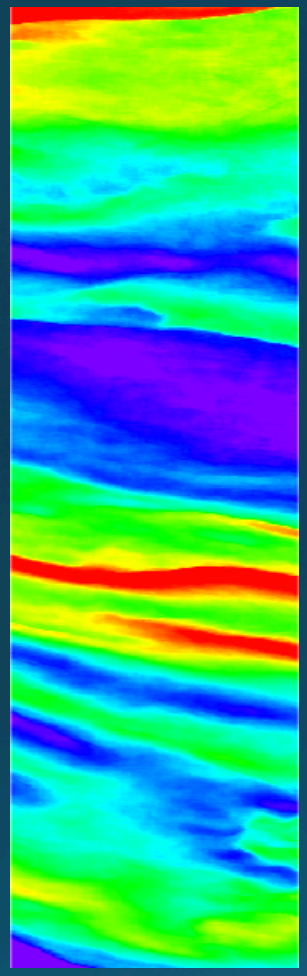

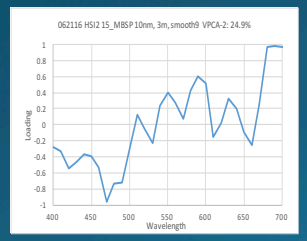

D) MTRI 6VPCA -3: 11.9%

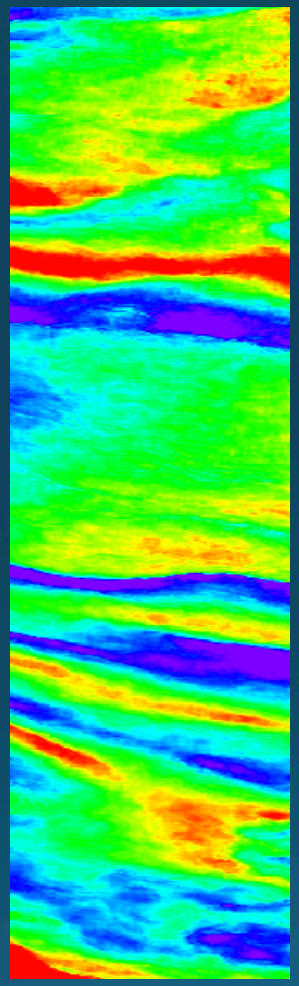

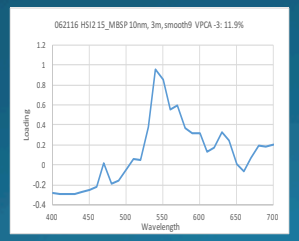

E) MTRI 6VPCA 4: 3.6%

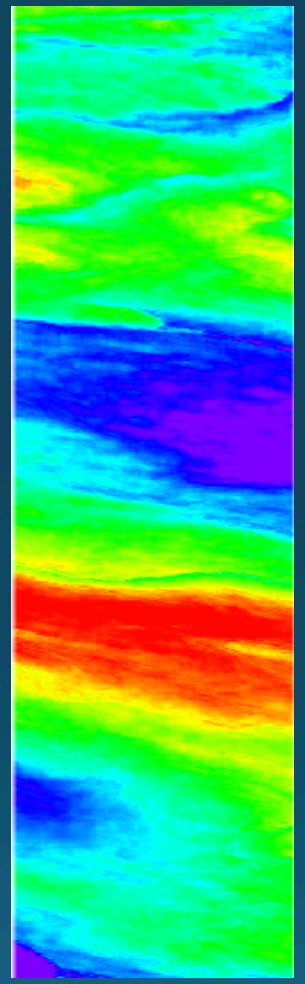

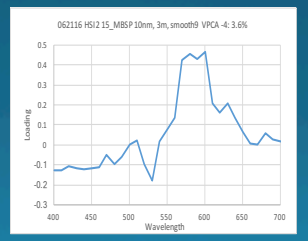

F) MTRI 6VPCA 5: 1.8%

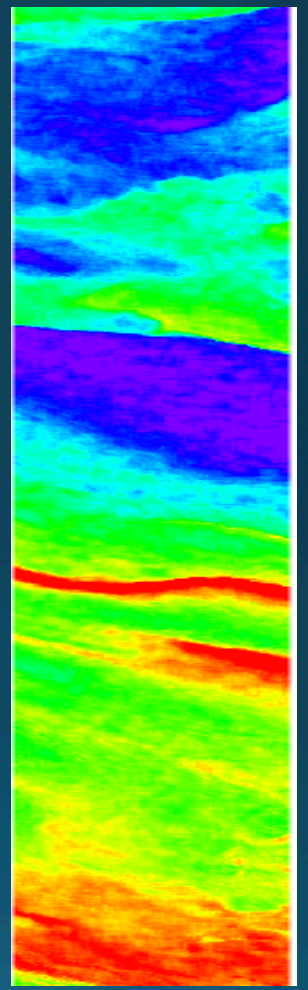

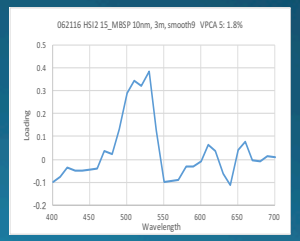

N

KSU Spectral Unmixing Experimental Outcome

Spectral Placement and Resolution	Number of Components extracted	
	30m	3m
Landsat 8: Four bands: 440, 480, 560, 655 @ 20, 60, 60 and 30 nm resolution	3	3
NASA HSI2: 31 Bands 400-700 nm @10nm resolution	5	5

Ortiz et al., (HyspIRI 2017; jortiz@kent.edu)

VPCA 1 Simulated L8 bands, 30m

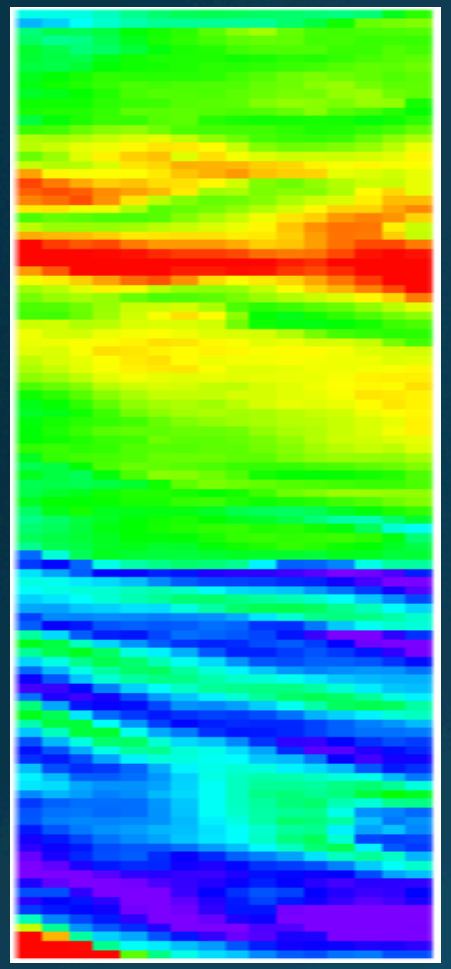

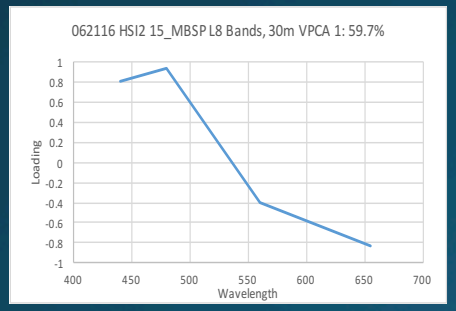

VPCA 1 Simulated L8 bands, 3m, Smooth 9x9

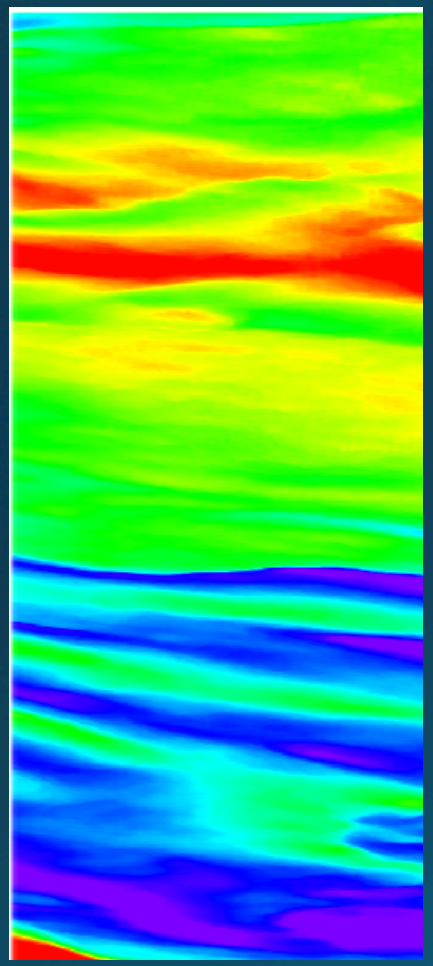

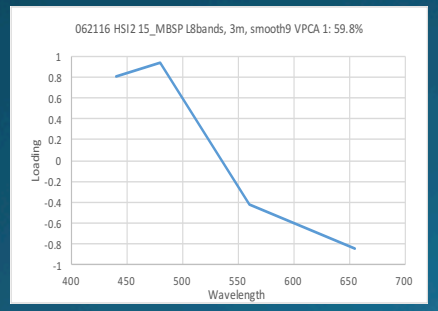

VPCA -1 HSI2 10nm, 30 m

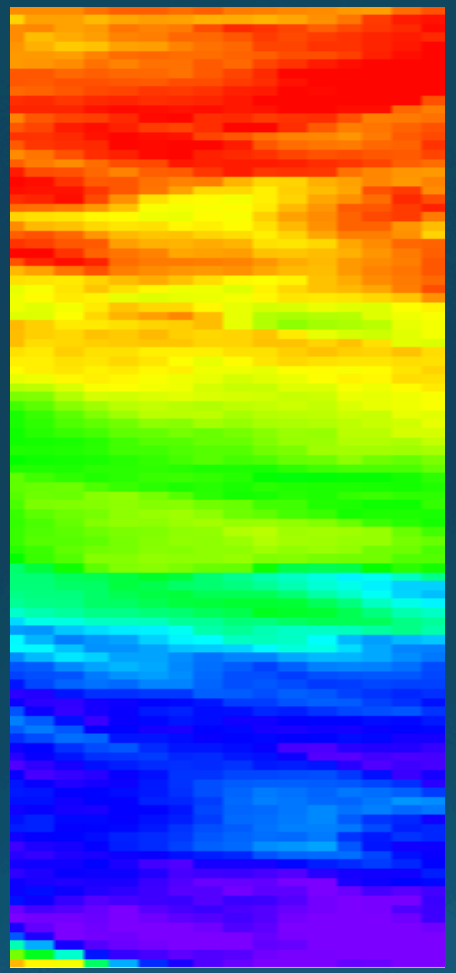

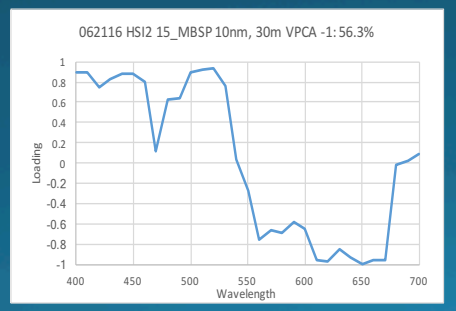

VPCA1 HSI2 10nm, 3 m, Smooth 9x9

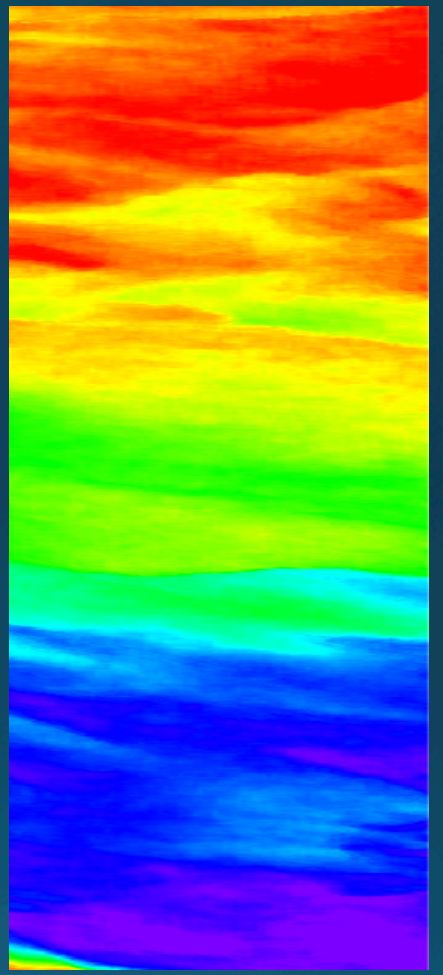

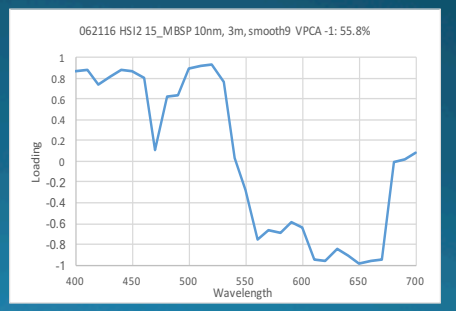

Composition:
Illite,
diatoms and
phycoerythrin
(R=0.94)

N

Ortiz et al., (HyspIRI 2017; jortiz@kent.edu)

VPCA 2 Simulated L8 bands, 30m

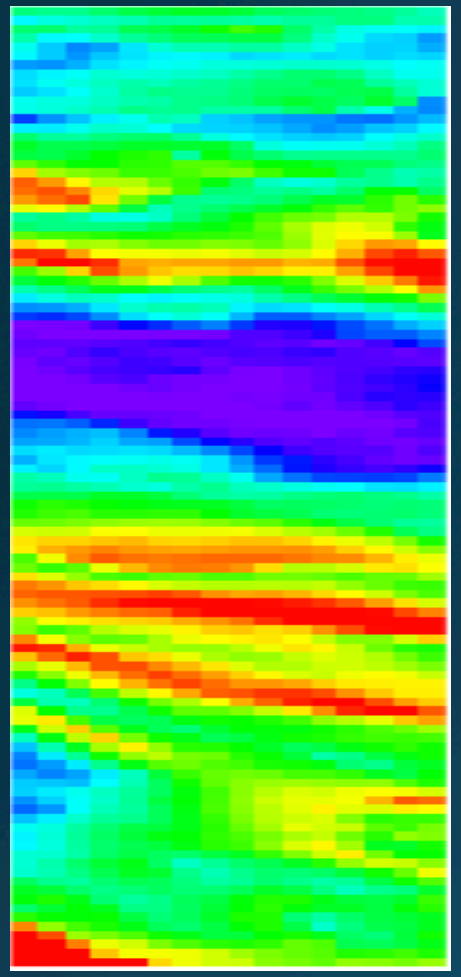

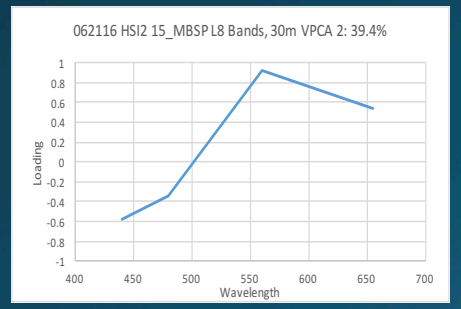

VPCA 2 Simulated L8 bands, 3m, Smooth 9x9

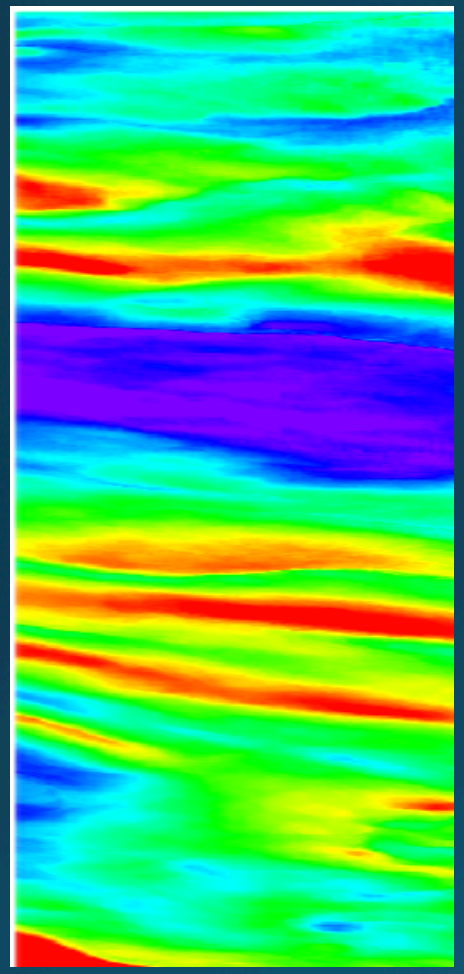

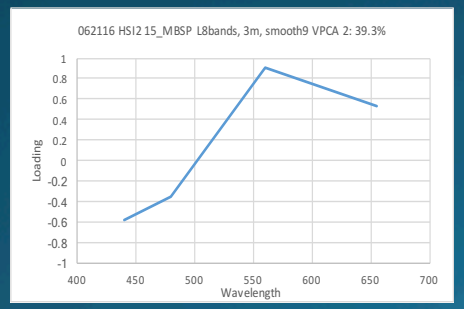

VPCA 2 HSI2 10nm, 30 m

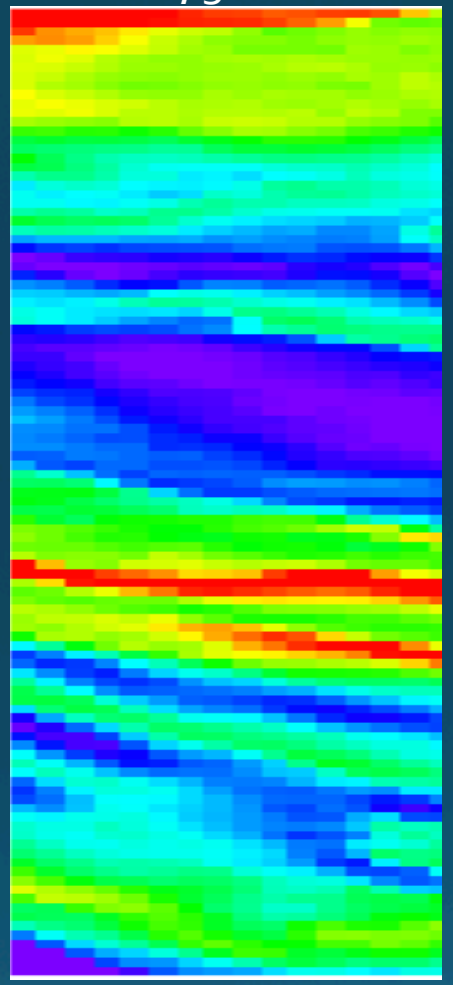

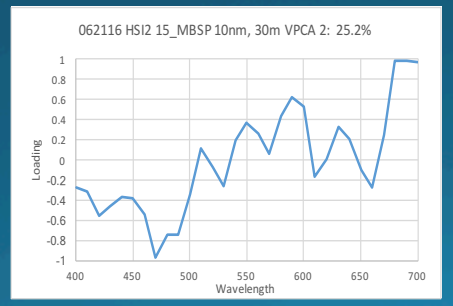

VPCA 2 HSI2 10nm, 3 m, Smooth 9x9

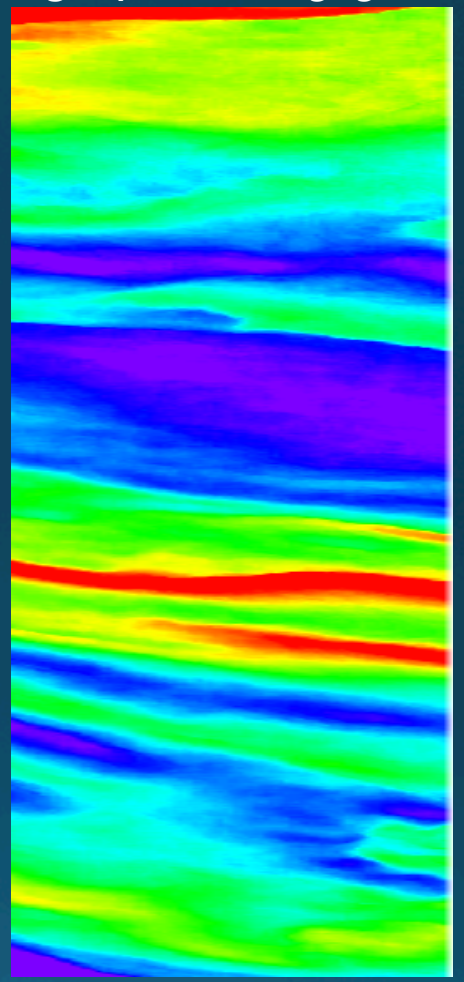

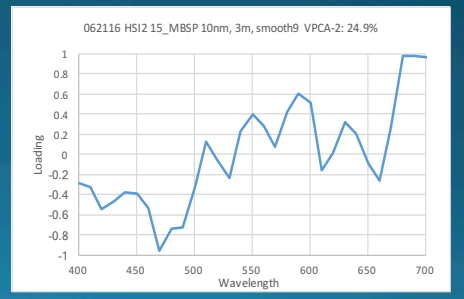

Composition: Haematite, Green algae, -α carotene and phycocyanin (R=0.90)

N

Ortiz et al., (HyspIRI 2017; jortiz@kent.edu)

VPCA 3 Simulated L8 bands, 30m

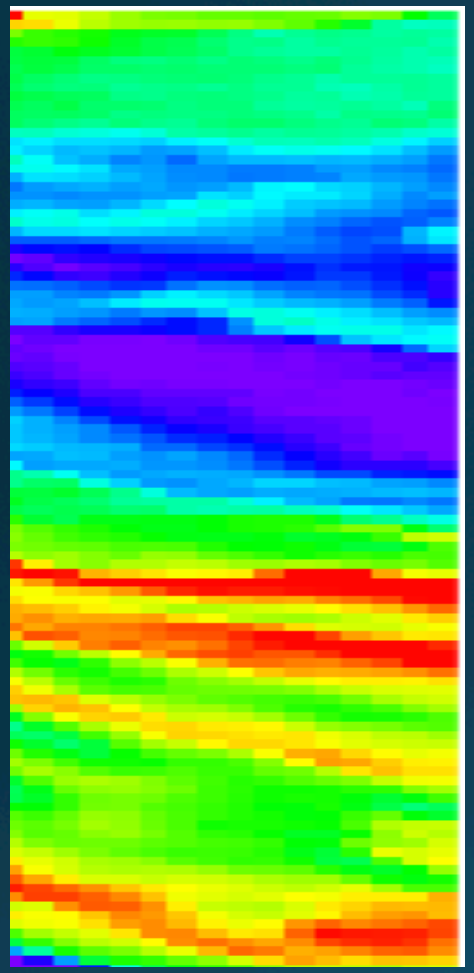

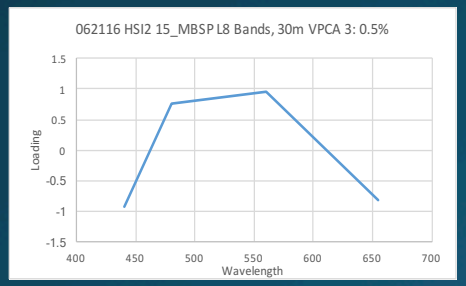

VPCA 3 Simulated L8 bands, 3m, smooth 9x9

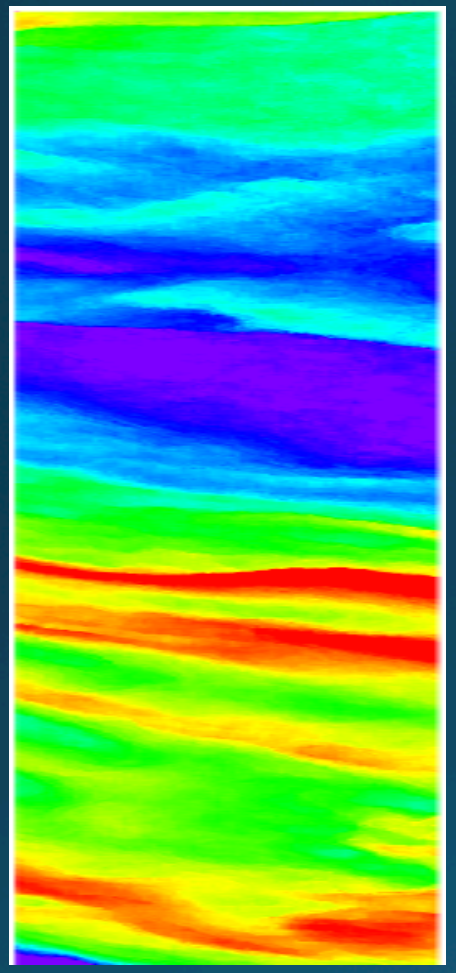

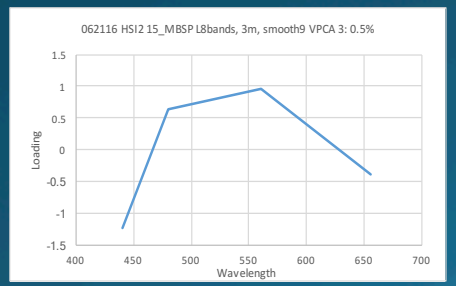

062116 15_MBSP 10nm, 30m, VPCA 3

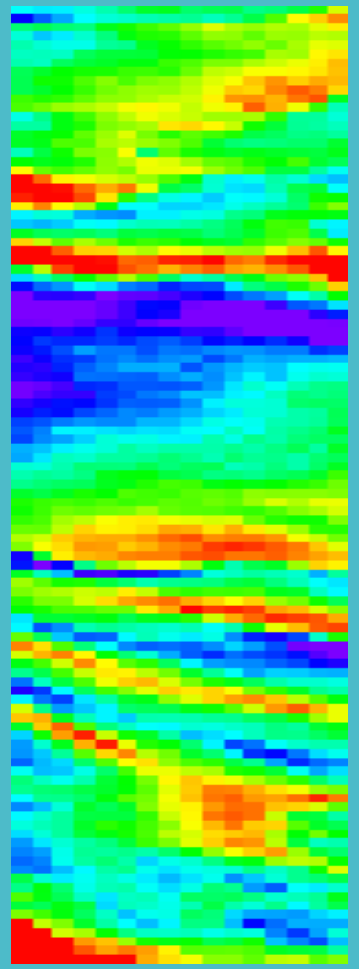

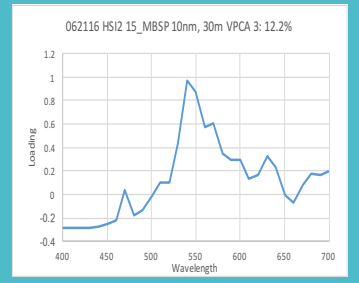

062116 15_MBSP 10nm, 30m, VPCA 4

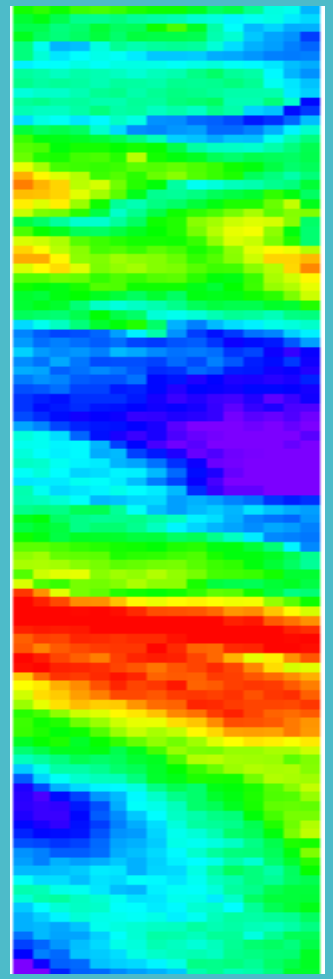

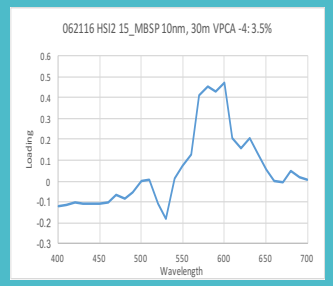

062116 15_MBSP 10nm, 3m, SM9 VPCA-3

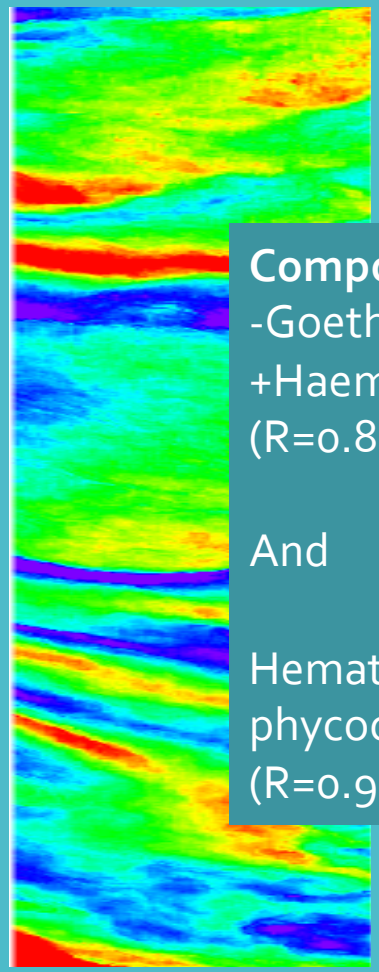

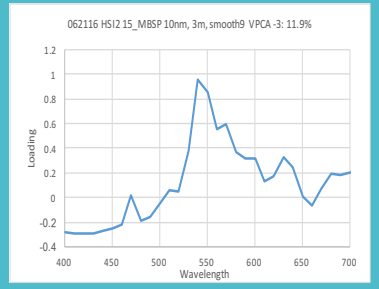

062116 15_MBSP 10nm, 3m, SM9, VPCA 4

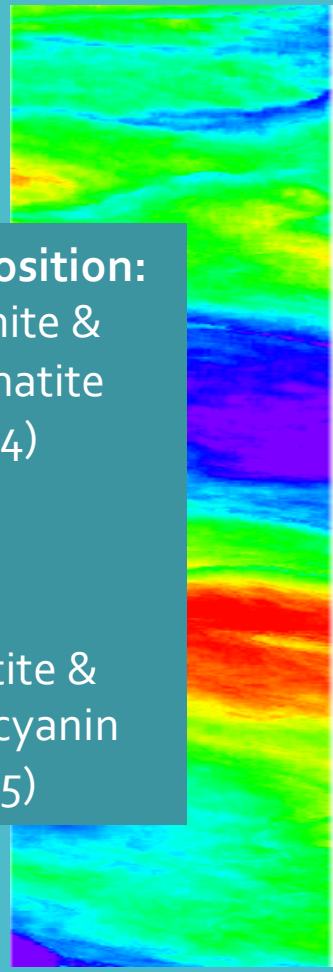

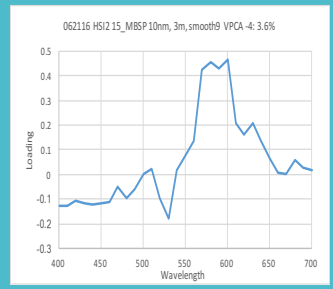

Composition:
-Goethite & +Haematite (R=0.84)

And

Hematite & phycocyanin (R=0.95)

Actual L8 Image Decomposition

061916 L8 (surface reflectance product), swath15 subset: VPCA decomposition

RGB

061916 L8 swath 15 subset VPCA 1FLIP

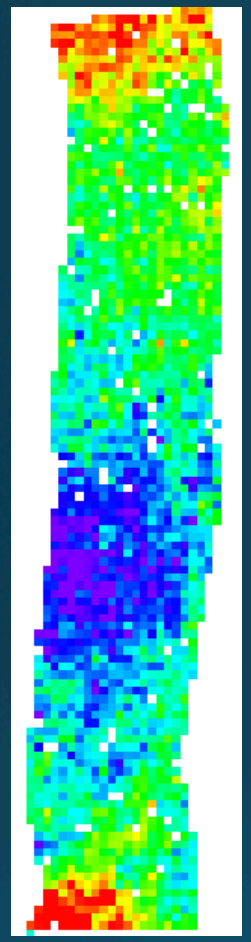

Composition:
Diatoms
(R=0.996)

N

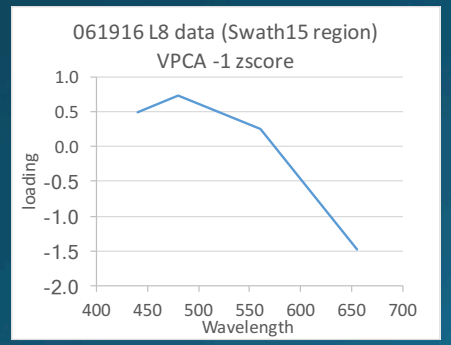

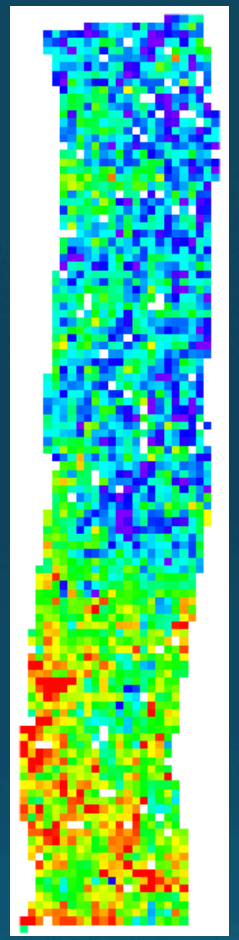

Composition:
Phycocyanin
(R=0.993)

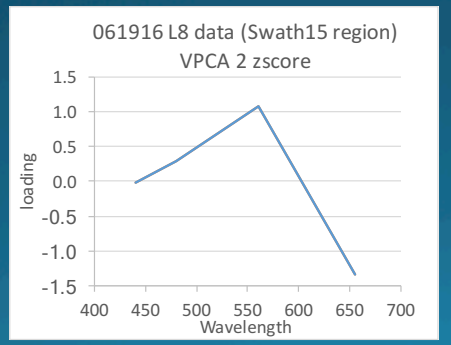

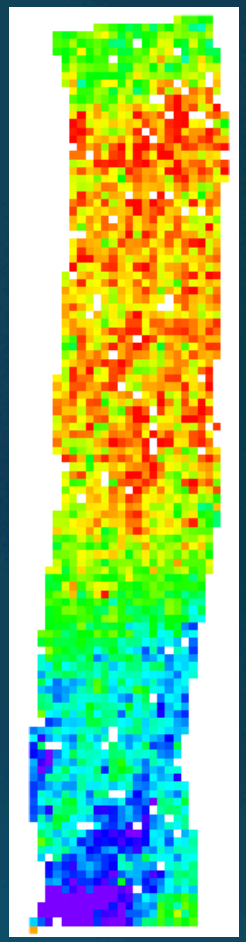

Composition:
Chl a &
carotenoids
(R=0.996)

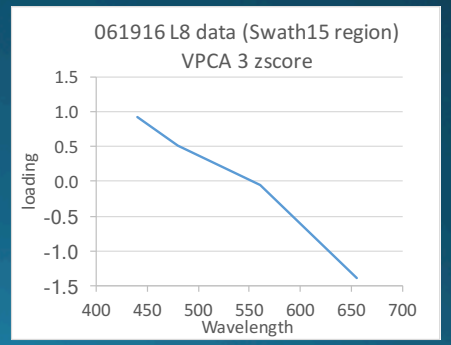

Ortiz et al., (HyspIRI 2017; jortiz@kent.edu)

Kent State Univ. Spectral Unmixing: 082317 S3A L2 Lake Erie VPCA Scores (J. Ortiz and D. Avouris)

Sentinel3A BOA

RGB

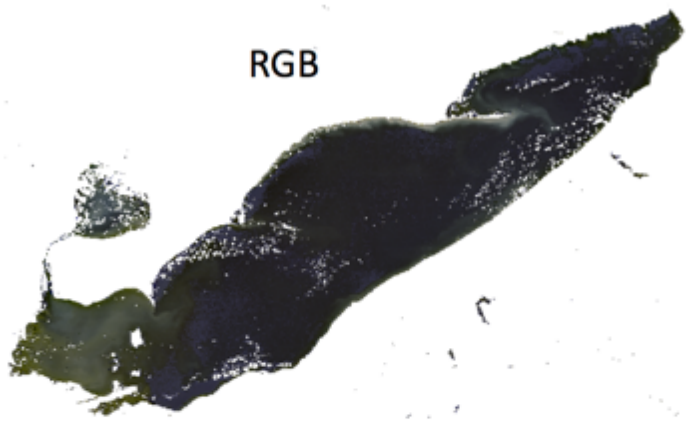

- Phycocyanin, - myxoxanthophyll

VPCA 1: 33.6%

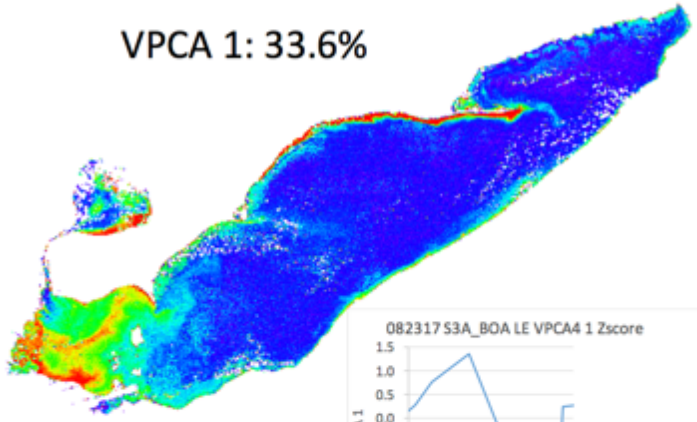

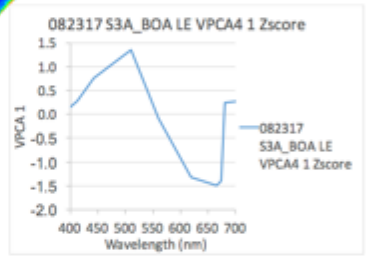

+ illite, + accessory pigment

VPCA 2: 32.4%

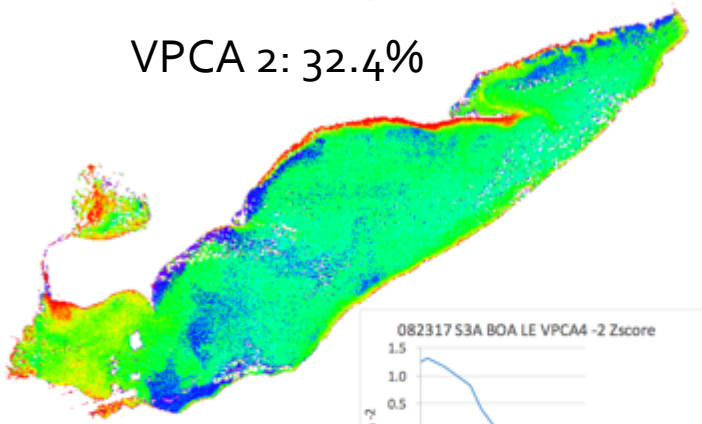

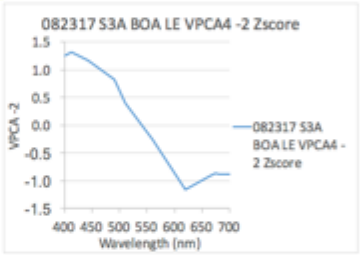

+ cyanobacteria

VPCA 3: 19.6%

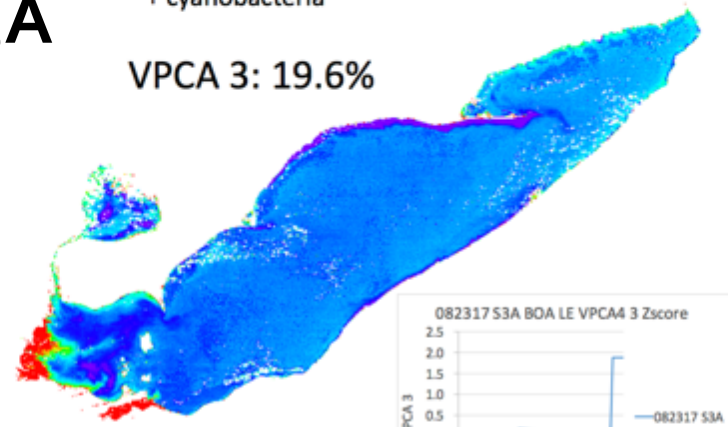

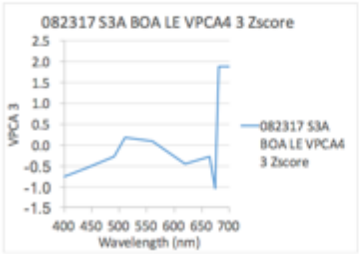

+ phycocyanin, -fucoxanthin

VPCA 4: 11%

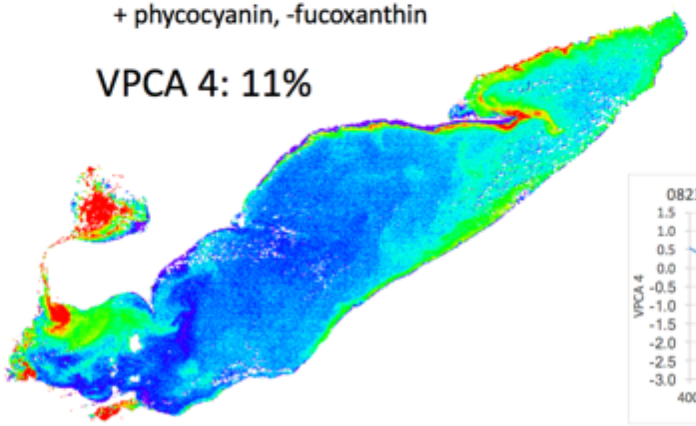

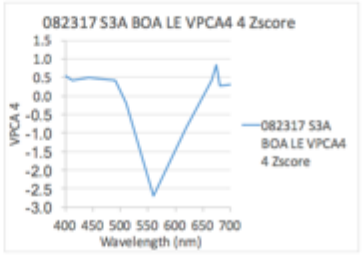

Ortiz et al., (HyspIRI 2017; jortiz@kent.edu)

Sentinel3A Comparison of VPCA to NOAA CI

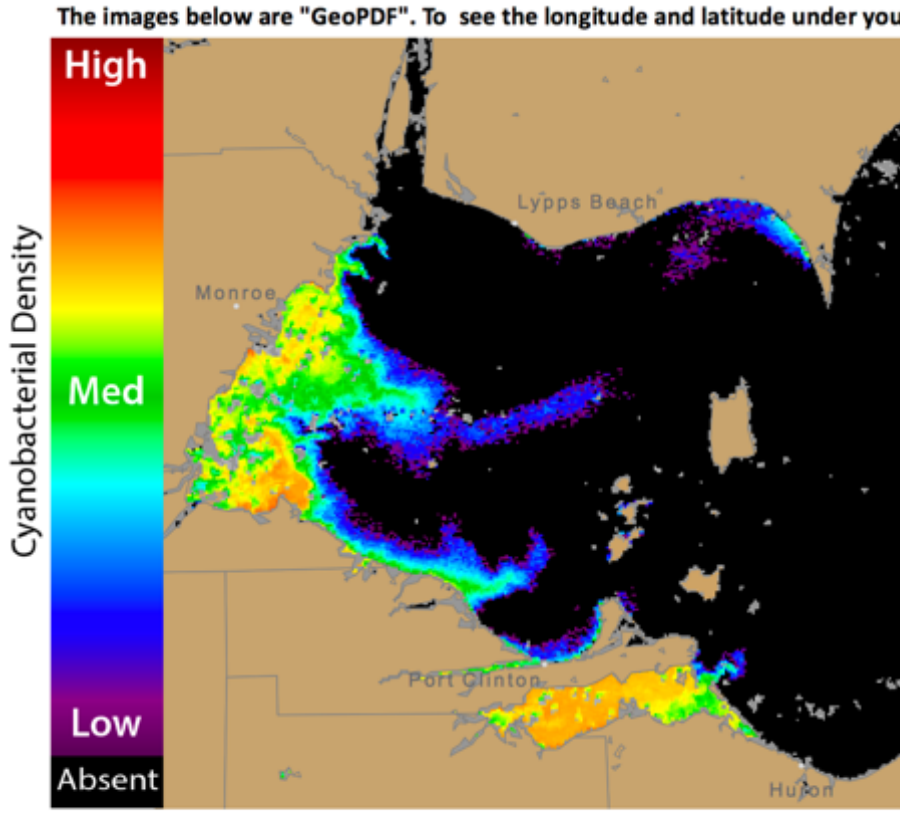

Figure 1. Cyanobacterial Index from modified Copernicus Sentinel 3 data colle
missing data. The estimated threshold for cyanobacteria detection is 20,000 cell

+ cyanobacteria

VPCA 3: 19.6%

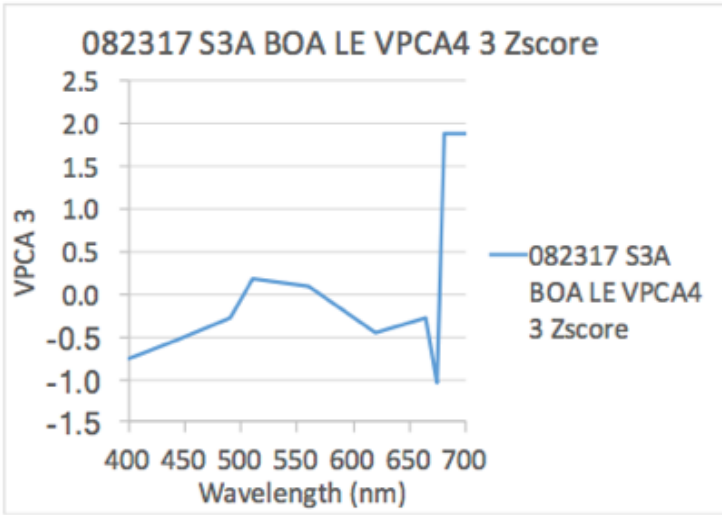

Ortiz et al., (HyspIRI 2017; jortiz@kent.edu)

Conclusions

1. VPCA ties optical assemblages to minerals, phytoplankton and cyanophyte phyla
2. KSU VPCA decomposition method can be applied successfully to Landsat, MODIS, HICO, NASA Glenn HSI2
3. VPCA is well suited for application to Sentinel-3, HyspIRI, PACE: Makes use of ***all*** information present in hyperspectral data
4. The NASA HSI2 (31 visible bands @ 10nm resolution) collects about twice as many components from a simulated L8 scene (with 4 bands in the visible)
5. Spectral decomposition of an actual L8 image collected within two days of the NASA HSI2 swath is consistent with the simulated results
6. Increasing spectral resolution doubles the information that can be partitioned in a scene in terms of the number of extractable components
7. Increasing spatial resolution provides more detailed images, but does not help to extract additional spectral components using this method

Ortiz et al., (HyspIRI 2017; jortiz@kent.edu)

Recent Publications

See Water quality webpage at: http://www.personal.kent.edu/~jortiz/home/wqr.html

Ortiz et al., Intercomparison of Approaches to the Empirical Line Method for Vicarious Hyperspectral Reflectance, Front. Mar. Sci., 14 September 2017 | https://doi.org/10.3389/fmars.2017.00296

KA Ali, **J.D.Ortiz**, N Bonini, M Shuman, C Sydow, Application of Aqua MODIS sensor data for estimating chlorophyll a in the turbid Case 2 waters of Lake Erie using bio-optical models, GIScience & Remote Sensing, 1-23, 2016

Ali, K.A., and **J.D. Ortiz**, Multivariate approach for chlorophyll-a and suspended matter retrievals in Case II waters using hyperspectral data, Hydrological Sciences Journal, 2016. DOI 10.1080/02626667.2014.964242.

GS Bullerjahn, et al., Global solutions to regional problems: Collecting global expertise to address the problem of harmful cyanobacterial blooms. A Lake Erie case study, Harmful Algae 54, 223-238, 2016

Ortiz, J.D., Witter, D.L., Ali, K.A., Fela, N., Duff, M., and Mills, L., Evaluating multiple color producing agents in Case II waters from Lake Erie, International Journal of Remote Sensing, 34 (24), 8854-8880, 2013.

Ali, K.A., Witter, D.L., and **J.D. Ortiz**, Application of empirical and semi-analytical algorithms to MERIS data for estimating chlorophyll a in Case waters of Lake Erie, Environmental Earth Sciences; DOI 10.1007/s12665-013-2814-0, published Oct 1, 2013.

Ali, K.A., Witter, D.L., and **J.D. Ortiz**, 2012, Multivariate approach to estimate color producing agents in Case 2 waters using first-derivative spectrophotometer data, Geocarto International, Early online release: 10/30/2012 DOI:10.1080/10106049.2012.743601.

Witter, D., **Ortiz, J.D.**, Palm, S. Heath, R., Budd, J., Assessing the Application of SeaWiFS Ocean Color Algorithms to Lake Erie, Journal of Great Lakes Research, 35, 361-370, 2009.